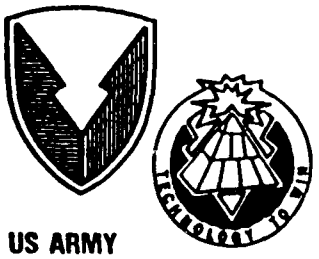

AD

MTL TR 89-7

A STUDY OF FRAGMENTATION DISPERSION MEASUREMENTS OF UNIQUE MULTILAYER FRAGMENTING STRUCTURE

January 1989

D. L. MYKKANEN
ETA Corporation
P.O. Box 6625
Orange, CA 92667

FINAL REPORT

Contract DAAG46-85-C-0078

Approved for public release; distribution unlimited.

Prepared for

U.S. ARMY MATERIALS TECHNOLOGY LABORATORY
Watertown, Massachusetts 02172-0001

AD

MTL TR 89-7

A STUDY OF FRAGMENTATION DISPERSION MEASUREMENTS OF UNIQUE MULTILAYER FRAGMENTING STRUCTURE

January 1989

D. L. MYKKANEN
ETA Corporation
P.O. Box 6625
Orange, CA 92667

FINAL REPORT

Contract DAAG46-85-C-0078

Prepared for

U.S. ARMY MATERIALS TECHNOLOGY LABORATORY
Watertown, Massachusetts 02172-0001

The findings in this report are not to be construed as an official Department of the Army position, unless so designated by other authorized documents.

Mention of any trade names or manufacturers in this report shall not be construed as advertising nor as an official indorsement or approval of such products or companies by the United States Government.

DISPOSITION INSTRUCTIONS

Destroy this report when it is no longer needed
Do not return it to the originator

FORWARD

This work was performed for the ARMY MATERIALS TECHNOLOGY LABORATORY, Watertown, MA. 20172, under contract DAAG46-85-C-0078 with Mr. J. F. Dignam as Project Manager and Dr. S. C. Chou as Contracting Officer Technical Representative. The support and guidance of Dr. S. C. Chou and J. F. Dignam is gratefully acknowledged.

TABLE OF CONTENTS

ILLUSTRATIONS

LIST OF TABLES

1.0 INTRODUCTION

1.1 BACKGROUND

In the past, conventional nonnuclear warheads for strategic defense systems have been contained as a separate subsystem within the warhead section. The warhead fragments are then explosively driven through the interceptor structure and heatshield toward the target. These separate systems result in a weight and performance penalty. The interceptor structural subsystem must be designed for minimum weight to efficiently survive the launch flight and blast environments while the warhead subsystem is designed for maximum fragment weight. Even with efficient design the structure is a weight penalty for the warhead. Combining the two subsystems achieves a system improvement. The structural design can incorporate enhanced stiffness and strength with no weight penalty. The fragments do not give up their kinetic energy penetrating the interceptor structure. In addition, the synergy allows for the original weight allotted to the structure to be included in the warhead, further increasing the total system performance.

Current concepts for fragmenting weapons without individual aiming or complex interleaving of explosives are limited to essentially chunky fragments which when exploded are found in a mono-layer expanding cloud of fragments in flight.

Penetration and internal damage would be enhanced if the fragment impacts are closely spaced causing interactions, such as side by side hits with interconnecting failures or if one wave of fragments penetrates the surface followed by a second wave of fragments which damage the internal structure. These benefits require either more accuracy for smaller miss distances or multiple layers of fragments with the same trajectory and close spacing in the fragment cloud.

These improvements can be achieved by creating a multi-layer cloud of fragments (possibly multiple layers) expanding from the exploded warhead. NNK single layered warheads would be improved if multiple layers were used to achieve closer spacing within the fragment cloud. In seeking an efficient method of stacking multiple layers of fragments, it is found that the most densely packed arrangement of geometric structures found in nature is a combination of tetrahedra and octahedra as shown in Figure 1.1. In crystalline structures these are called close-packed hexagonal or face centered cubic. This construction of tetrahedra and octahedra has interesting characteristics. The tetrahedron is a minimum volume or mass unit cell with a maximum number of edges and corners. Structurally, its edges are ideally the most stable minimum mass truss construction. The tetrahedron can be considered to be the "sharpest" chunky fragment possible. The octahedron in the structure contains eight sides, each of which is the triangle, and four times the volume or mass of four-sided tetrahedron. The octahedron, thus, is a more massive and rounded chunky fragment. These two geometric natural structures can be fabricated as fragments by creating a skin or separation plane on one or both of the geometric volumes.

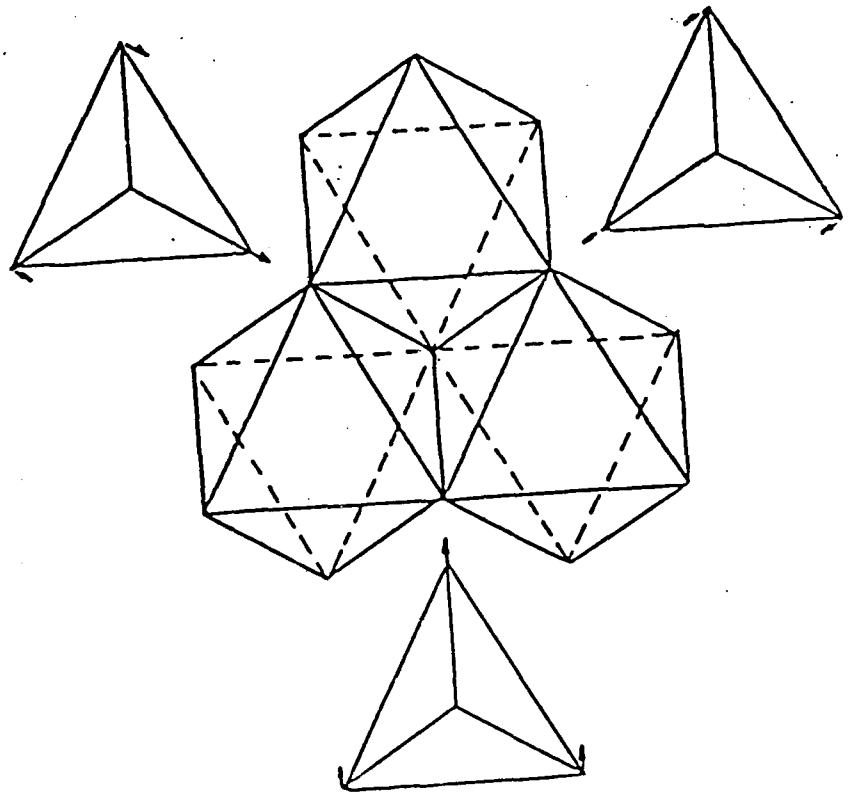

Figure 1.1 GEOMETRIC STRUCTURES

In addition, since it is desired that the fragments have the same mass, the octahedron can be divided into subunits having the same mass as the tetrahedron with a portion of the octahedral volume used as separation plane or skin.

The development activities for this new and novel multilayered fragmenting warhead concept were carried out with a technically conservative approach. The analytical studies* have shown a potential benefit from combining the fragments of the warhead and the structural system to be at least a 12% increase in energy in the fragment. The structural property tests* have shown that the potential mechanical properties will meet the design requirements. The current effort is to determine the fragmentation characteristics of the integrated structural concept. This involved designing and fabricating test specimens to show the fragmentation mechanism and potential benefits of the concept. The cylindrical design is closely related to the structural test specimens used before to maintain the continuity of the evaluation program.

* Mykkanen, D. L.,"DEVELOPMENT AND CHARACTERIZATION OF MULTILAYER INTEGRATED WARHEAD STRUCTURE", AMMRC TR 85-10 (May 1985)

1.2 PROGRAM TECHNICAL OBJECTIVES

This program was carried out to demonstrate the feasibility of this unique multilayer fragmenting structural concept. The demonstration was planned as an experimental and analytical program. The mechanical properties predicted by the analytical model were to be compared with the measurement of these properties. The experimental results would be used to establish the feasibility.

In order to accomplish a lower cost development the early tests were to be carried out using substitute or surrogate materials. The surrogate materials development program provided low cost guidance for the tooling design and casting approaches for the final steel castings. When the surrogate manufacturing processes and procedures were evaluated and the surrogate composite properties measured, the final high temperature investment casting development efforts and property measurements would be accomplished using a high strength castable stainless steel. Casting and characterizing the steel flat plate concepts demonstrated the good structural properties of the integrated fragmenting warhead concept and provided the need to proceed to the cylindrical test program.

2.0 TECHNICAL ACTIVITIES

This testing program was accomplished in two phases. The first was a preliminary test of flat plates to establish the feasibility of fragmentating the concept. The second involved the designing, fabricating and testing of the cylindrical test specimens.

2.1 FLAT PLAT TESTS

This test program used castings available from a previous test program and a simple test program. The test plates were mounted above a catcher, fragmented by the d.e.t.a. explosive, and the fragments were caught with multi-layers of soft particle board. Even though the two plates where severely flawed during casting, they did give insight into the mechanism of fragmentation. After reassembling the plates and examining the fragments, a better understanding of the relationships between core assembly and the fragmentation mechanism was obtained. As discussed in the following sections, the test showed that the integrated structure/warhead concept will fragment and the data provides guidance for the design of future test specimens and tests.

2.1.1 FLAT PLATE TEST OBJECTIVES

The objective of this program was to investigate the mechanisms of fragmentation and possible problems when flat plate specimens of this unique construction were exposed to sheet explosives. The concept showed exceptional strength and stiffness in the previous test program and these tests were to provide a quick look at the feasibility of the fragmenting concept.

2.1.2 TEST PROCEDURE

This was to be accomplished by using previously manufactured castings No. 8 and 12 from an earlier program and was intended to provide guidance for further testing of this type. The explosive was cut, weighed, and taped to the top of the test specimen. The specimen and explosive were then taped to the support structure as shown in Figure 2.1. The plates were suspended approximately four feet above the particle boards by a wooden truss. The initiator was mounted in a small annular ring starter charge as shown in Figure 2.2.

The initiator was placed approximately 1/2 in. from the core assembly on the solid cast end of the specimen. It was expected that the explosive wave would have reached steady state by the time it reached the core assembly. The results suggested that the explosive pressure load vector may have been at an angle to the surface other than normal, resulting in a bending moment in the specimen. This was observed in some of the fragmented pieces. This also could have been the result of the inertial changes from the massive cast ends to the core area in the center. The pressure wave was observed to provide an asymmetry to the fragmenting of the plates.

Figure 2.1 TEST SPECIMEN

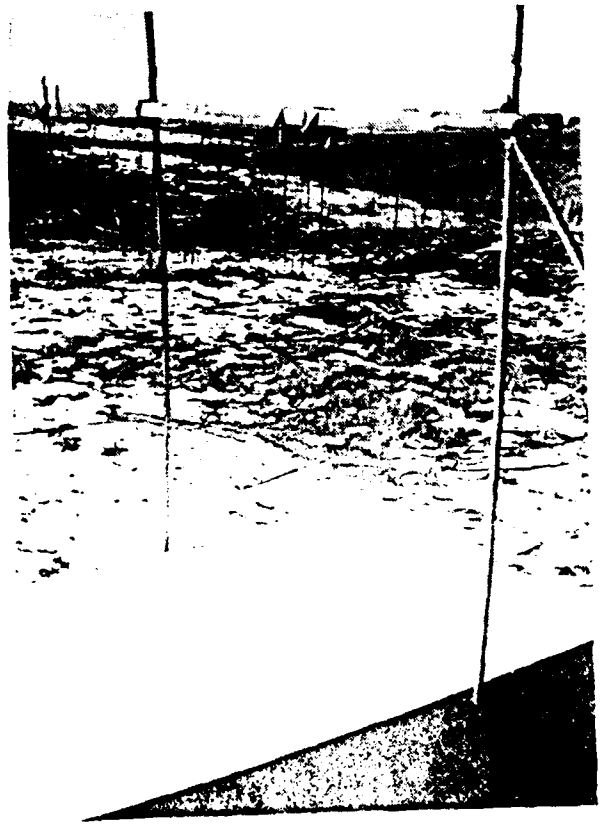

Figure 2.2 TEST SUPPORT STRUCTURE

The first test was carried out on Casting No. 12. One 171 gm. sheet of C5 deta sheet (.927 x 9.53 x 13.65 cm) (0.365 x 3 3/4 x 5 3/8 in.) was taped to the specimen and mounted in the manner shown in Figure 2.1 and 2.2. The initiator was placed in the annular ring and the area cleared. The explosive was fired driving the casting and its fragments into the particle board catcher below the specimen. The fragments were observed to scatter radially as shown in Figure 2.3. The large holes were the result of the massive casting ends being driven into the catcher boards. The fragments were collected from the boards. Most of the fragments were recovered as shown in Figure 2.4. After further evaluation it appeared that some of the fragments missed the boards and were not recovered.

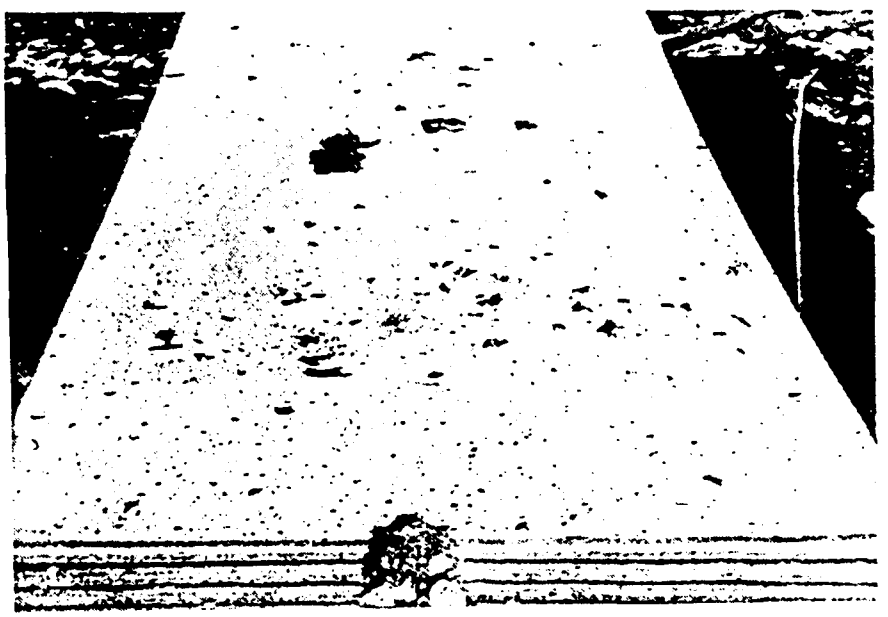

Figure 2.3 FRAGMENT DISTRIBUTION FROM CASTING NO. 12

The fragments observed in Figure 2.4 showed that a number of tetrahedron and half-octahedrons were still connected and thus the fragmentation was not as complete as desired. It was decided to increase (double) the charge to mass ratio in the hopes of achieving more complete fragmentation.

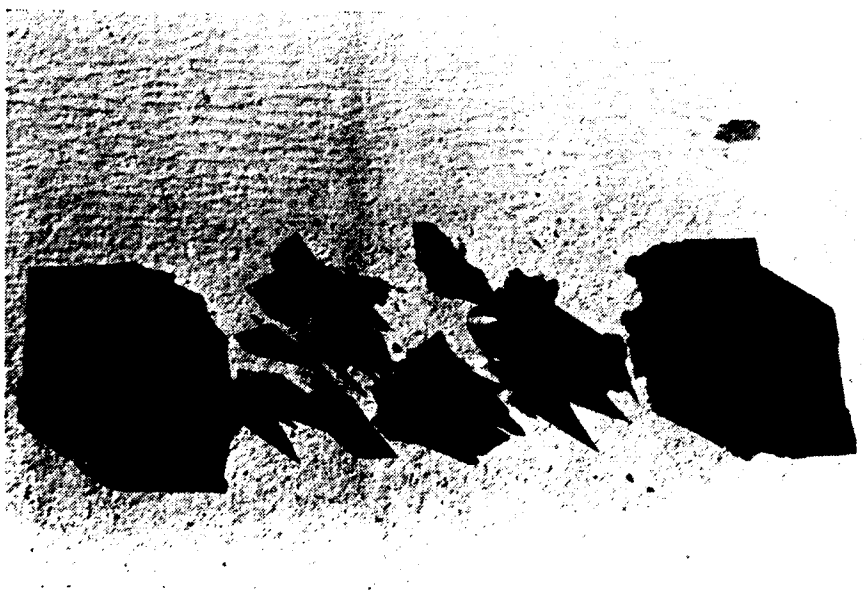

Figure 2.4 FRAGMENTS AND END PIECES FROM CASTING NO. 12.

In the same manner casting no. 8 was assembled with 3 sheets of explosive. One 171 gm. sheet of C5 (0.365 x 3 3/4 x 5 3/8 in.)(.927 x 9.53 x 13.65 cm) and two 100 gm. sheets of C1 deta sheet (0.195 x 3 3/4 x 5 3/8 in.)(0.495 x 9.53 x 13.65 cm) were stacked and assembled as before in Figure 2.1 and 2.2. The higher charge to mass ratio (approximately 0.015) resulted in the fragments being driven deeper into the catcher boards. Some penetrated through 5 sheets of 18 lbs/ft3 particle board. The radial scattering was greater than for casting 12 and more of the fragments did not hit the catcher sheets. An attempt was made to gather all of the fragments from the soil in the area near the boards. The gathered fragments are shown in Figure 2.5.

Figure 2.5 FRAGMENTS FROM CASTING NO. 8

The fragmentation was more complete than with casting 12 but it was still not total. Only a few pairs of a tetrahedron joined with a half octahedron did not fragment. The test pieces were bagged and returned to the laboratory for evaluation. The specimens were carefully evaluated in the laboratory in the attempt to explain the phenomena.

2.1.3 TEST RESULTS

Casting No. 12

The fragments and ends from Casting No. 12 were examined and reassembled in their relative locations as shown in Figure 2.6. Figures 2.6a and 2.6b show that some of the edge pieces had not been recovered. The reassembled samples showed the flawed fragments in which the core had penetrated the surface resulting in an area without a continuous skin. This casting had originally been rejected because the flaws were in the center of the bottom (2.6b) and at the edges of the top resulting in possible non-uniform skin across the total sample.

The indentation on the explosive side of the specimen was significant. Examination suggested that the initiator may have distorted the explosive wave. Some of the fragmentation suggested a bending action resulting from the relative accelerations as the explosive pressure wave traversed the mass discontinuity from the massive end to the core area.

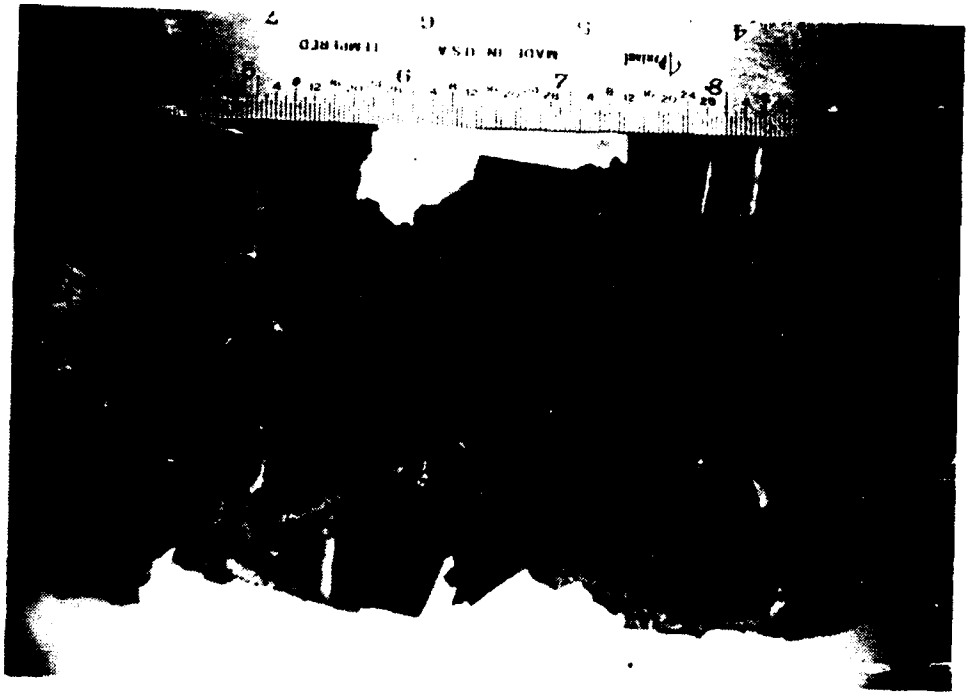

Figure 2.6a EXPLOSIVE SIDE OF FRAGMENTED CASTING NO. 12

Figure 2.6b OPPOSITE SIDE OF CASTING NO. 12

The fragments which did not separate showed extensive shear banding and partial separation (2.6b). This suggested that the charge to mass was near the fragmentation threshold level. The joined fragments were found on both the explosive and opposite side suggesting that the incomplete fragmentation is a geometry problem rather than an explosive problem.

The incomplete fragmentation of Casting No.12 was not entirely due to insufficient explosive. Casting flaws created thick and thin portions on opposite sides in the skin. Hence, the non-uniform section in core skin may have in part resulted in the non-uniform failures. In addition, the mass distribution between the core area and the casting's end pieces set up large inertial differences which may have been great enough to result in failures, where otherwise they would not have occurred, and cause incipient failures in areas which would have been expected to fail. This is suggested by the thickness data. The incipient fractures skin thicknesses ranged from 0.071 - 0.102 in. and the skin of the fragments that fractured ranged from 0.0 - 0.2 in. thick. There was no obvious thickness which resulted in fracture or survival in casting 12 and it is possible that position, with respect to the inertial transitions, was possibly more important than skin thickness. However, it was noticed that all incipient fractures observed had skin thickness which measured greater than 0.06 in. (the design skin thickness).

Casting No. 8

The fragments and ends from Casting No. 8 were examined and reassembled in their relative locations as shown in Figure 2.7. Figures 2.7a and 2.7b show that some of the edge pieces had not been recovered.

The reassembled samples showed that more fragmentation occurred in Casting No. 8 than in Casting No. 12. The mass discontinuity at the ends of the specimen did not seem as significant as with the thinner sheet explosive. As with Casting No. 12, there were tetrahedron/half octahedron twins. Often these were partially fragmented as shown in Figure 2.8.

By using more explosive on Casting No. 8 the problems with variations in skin thickness and possible inertial effect had been overcome. Yet, some of tetrahedrons did not completely separate from the adjacent half octahedron. This could have been the result of the casting flaws. It was noticed that when complete fragmentation did occur, it was associated with a well formed tetrahedron. That is, one that was attached to both skins. Those tetrahedrons, that because of casting nonuniformities that were not well attached to both skins, tended to have fragmentation cracks that progressed part of the way across the skin and stopped about half way to the next tetrahedron as shown in Figure 2.8.

The difference between separation and incomplete separation appears to be related to the continuity of the tetrahedron and the skin on both sides. Figure 2.9 shows a partially completed separation in which the cracked side had a well defined tetrahedron attached to both skins. Whereas, the uncracked side had little if any connection to the opposite skin as shown in Figure 2.10.

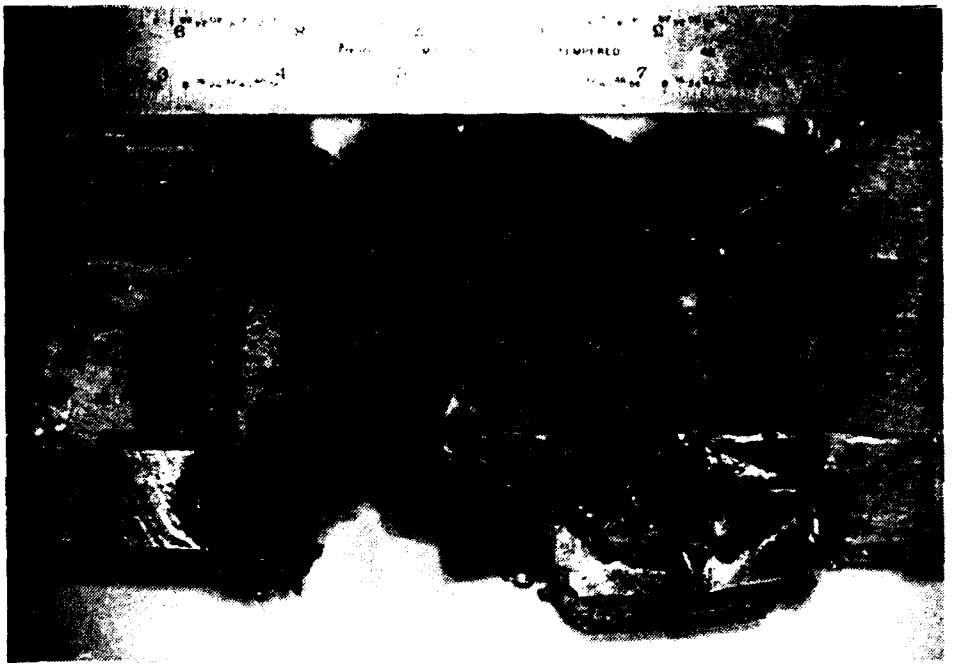

Figure 2.7a EXPLOSIVE SIDE OF FRAGMENTED CASTING NO. 8

Figure 2.7b OPPOSITE SIDE OF CASTING NO. 8

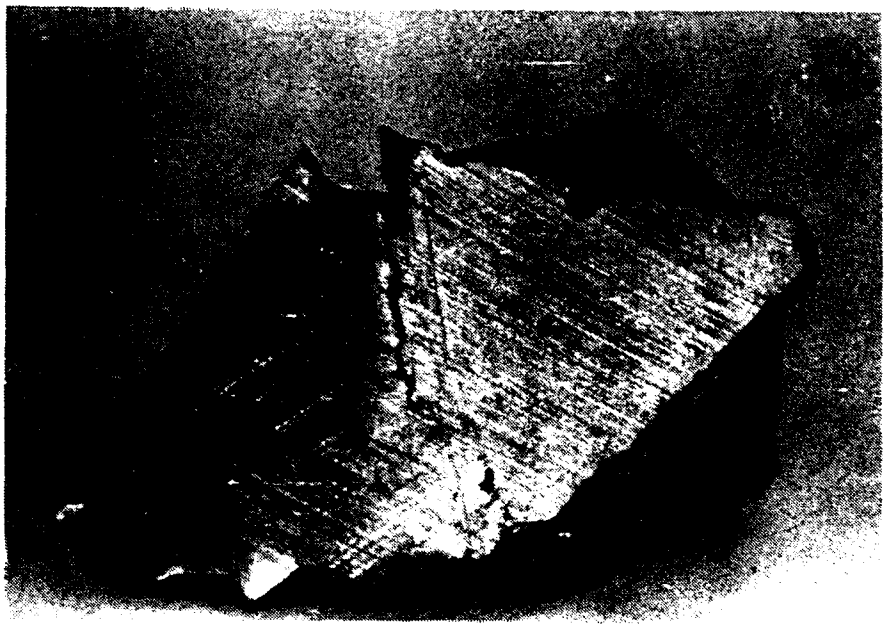

Figure 2.8 PARTIAL SEPARATION OD A TETRAHEDRON/HALF OCTAHEDRON

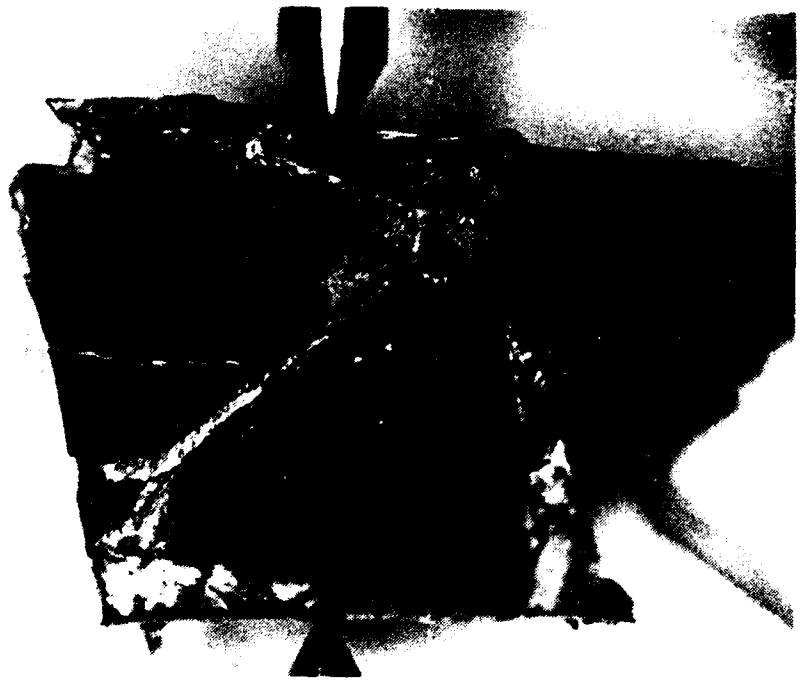

Figure 2-9 COMPLETE FRAGMENTATION AND RELATED COMPLETE TETRAHEDRON

Casting
Flaw

Figure 2.10 INCOMPLETE FRAGMENTATION AND INCOMPLETE TETRAHEDRON

This phenomena was observed on both sides of Casting No. 8 and is believed to be related to the fragmenting mechanism. The tetrahedrons carry the explosive load from one skin to the opposite skin, thereby providing the uniform shear loads which fracture both skins.

3.0 CYLINDRICAL TESTS

3.1 DESCRIPTION OF TEST WARHEADS

The original contract involved the fabrication and testing of 12 multilayered integrated structures. However, as a result of cost constraints, this was limited to two steel castings machined to complete warheads.

3.1.1 TEST SPECIMEN FABRICATION

The cylindrical test specimen involves changing the flat plate system used previously to a core system based upon cylindrical coordinates. The flat plate core design based upon individual single cavity ceramic cores was modified to an axial core which would extend from one end of the cylinder to the other and include both inner and outer fragment cavities. A sample of this type of core is shown in Figure 3-1. The fragments that would be generated are shown in Figure 3-2. This core concept is a complex three dimensional ceramic structure which is difficult to visualize and possible difficult to fabricate.

Tooling contractors were requested to quote on fabricating the tooling and the resultant cores. The responses were either rejections or not acceptable for cost or schedule considerations and another approach was selected.

It was decided to proceed using a modification to the flat-plate approach to fabricating cores. The cores were assembled into the cylindrical equivalent of polygons with the individual cores assembled as axial segments of the polygons. These segments were then rotated with respect the next segment in order to be able to machine cylinders from the polygons as shown in Figure 3-3.

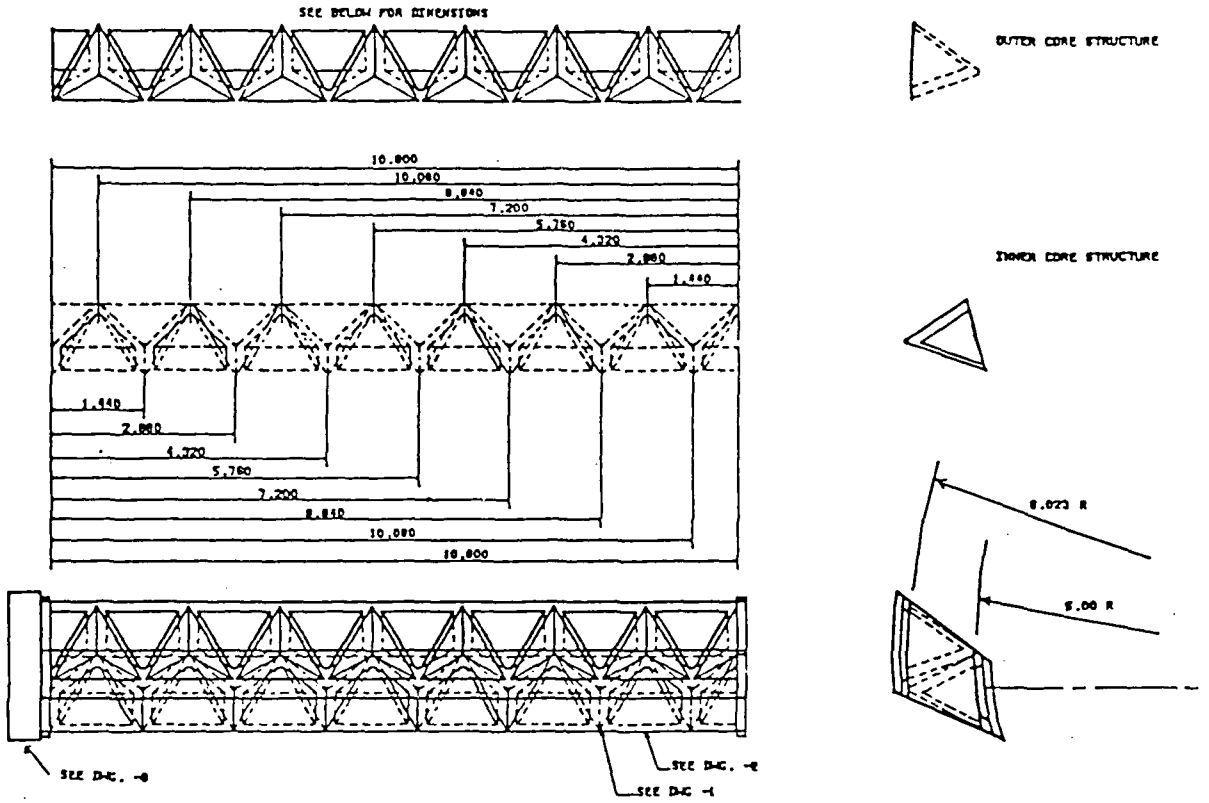

Figure 3-1 CYLINDRICAL PREFORM ASSEMBLY SEGMENTS

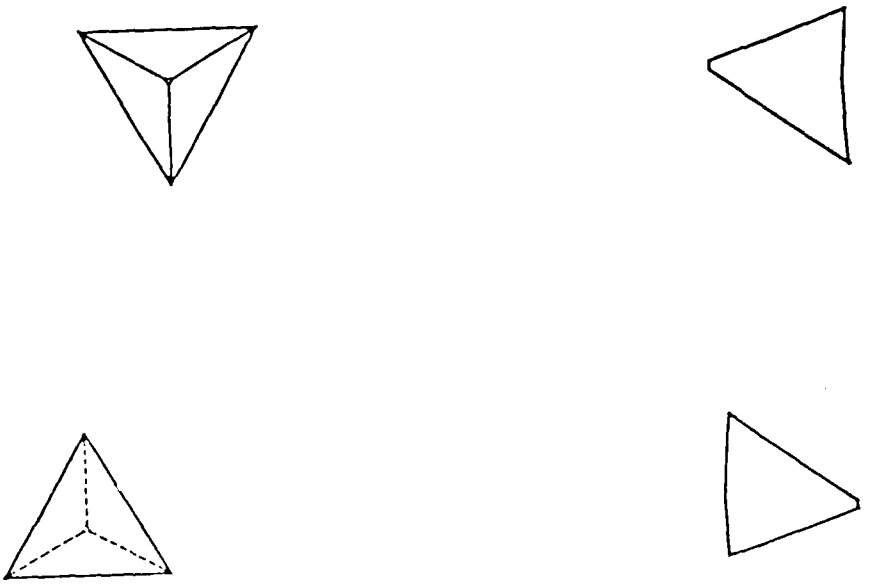

Figure 3-2a CYLINDRICAL TETRAHEDRAL CORE FRAGMENTS

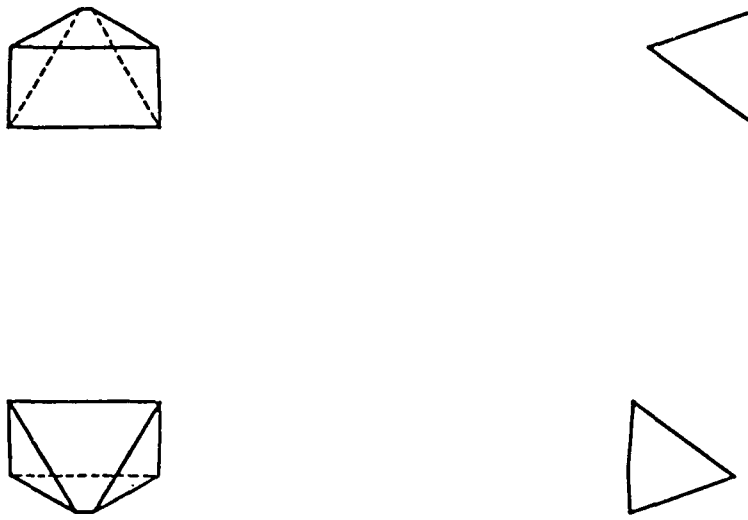

Figure 3-2b CYLINDRICAL HALF OCTAHEDRAL CORE FRAGMENTS

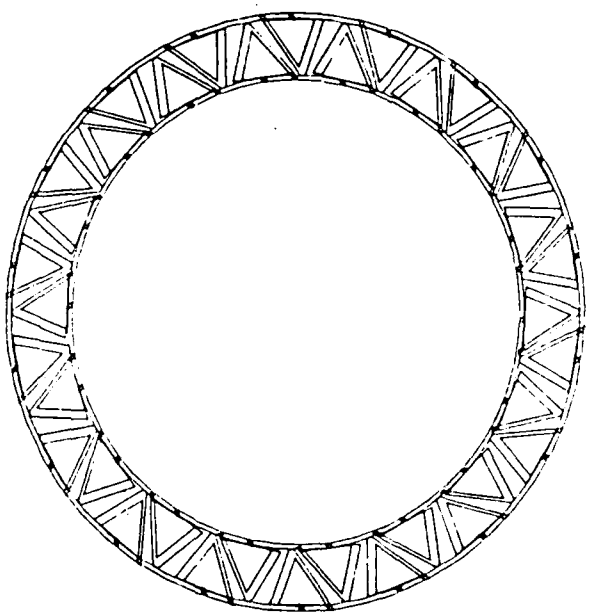

Figure 3-3 WARHEAD CYLINDER DESIGN

The concept of a structural skin was compromised but only at small areas in the skin not in continuously linear skin thickness reductions. This was expected to be an acceptable defect.

It was decided to proceed to fabricate a twelve (12) sided polygon using axial segments based upon the flat plate core structures. These cores were modified slightly to create a thicker skin to allow the machining of a cylinder from the polygon. This was a minor cost and schedule tooling change.

The wax-segment preforms are composed of six individual cores assembled into a strip in a mold and cast in place using wax as shown in Figure 3-4(a). These wax-segments are assembled into an arc-segment by combining two wax-segments and casting a wedge of ceramic to separate the segments and form a portion of the cylinder as shown in Figure 3-4(b). These arc-segments are then assembled into a polygon which is modified to approach a cylinder as shown in Figure 3-4(c).

The fabrication procedure consisted of assembling rows of ceramic cores in a wedge cavity which formed a segment. The cavity and its cores was then cast full with wax. The wax located the cores in position and supported the cores for handling and further assembly. Two segments were then assembled in another cavity and a ceramic wedge was cast to join the inner and outer cores and form a segment of a preform. The segments were assembled on wax-twelve-sided rings and cast in place to form the preform assemblies for the foundry as shown in Figure 3-5.

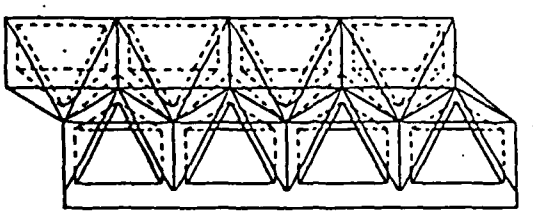

CORE CONCEPT

Figure 3-4a WAX SEGMENT PREFORMS

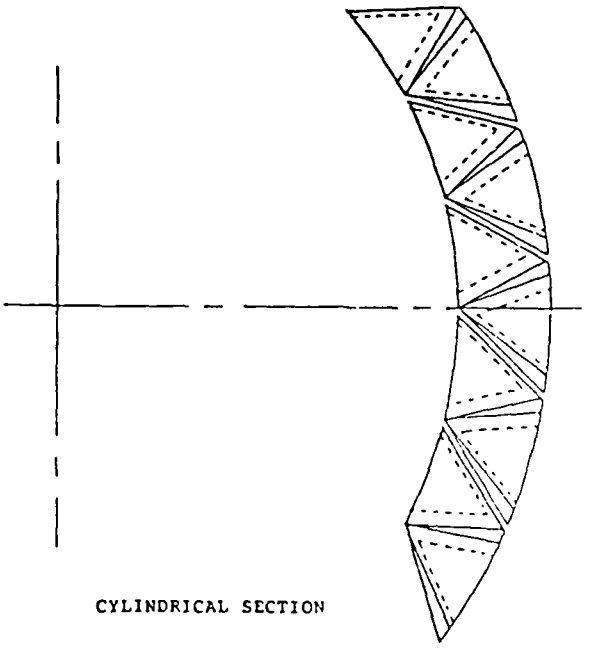

CYLINDRICAL SECTION

Figure 3-4b ARC SEGMENT PREFORMS

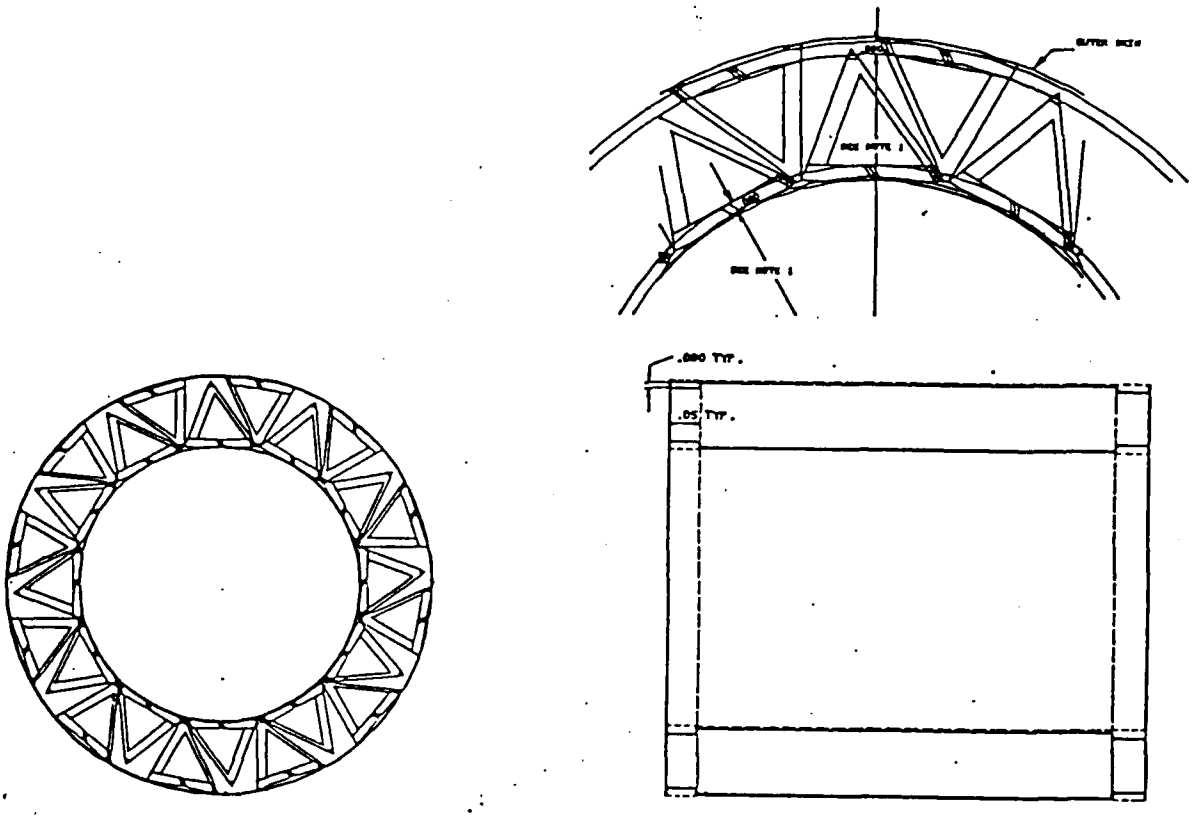

Figure 3-4c CYLINDER PREFORMS

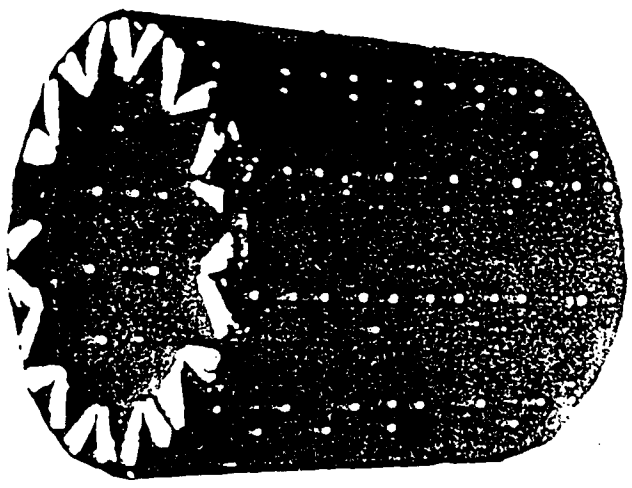

Figure 3-5 WAX PREFORM FOR FOUNDRY

A twelve-sided polygon has mirror symmetry which makes fabrication and inspection of the preform and casting easier. Sufficient wax segments were completed to assemble the full 12 cylindrical samples (based on twelve-sided polygons). These arc segments were characterized and mapped for each of the casting preforms. They were marked as to their position as inner or outer layer fragments and traceability was established.

First, a single prototype cylindrical casting was attempted. The wax preform was sent to an investment casting foundry where gates were attached and it was dip coated with ceramic. The ceramic was dried and the wax melted and drained from the ceramic casing leaving an empty cavity. A melt of 17-4PH steel was cast in the ceramic mold cavity to form the prototype. The ceramic coating was tailored to match the expected expansion of the ceramic cores in the preform. The ceramic cores in the preform shown in Figure 3-5 expanded more along the axial direction than estimated and the ends of the ceramic mold failed, losing a thin radial sheet of steel. This flash of steel was ground off and the visual and x-ray inspection of the casting showed it to be acceptable. Figure 3-6a shows the as cast polygon modified cylinder. It was then machined as shown in Figure 3-6b, and inspection showed it to be an acceptable explosive test specimen. Then a second preform was submitted to the foundry for casting. This casting was also acceptable and was machined as a test specimen.

Each of the two warhead castings selectef for testing were fabricated with cores which were traced to the original arc segments. The arc segments were scribed on the surfaces of the arc segments in the final casting to provide traceablity to the exploded fragments.

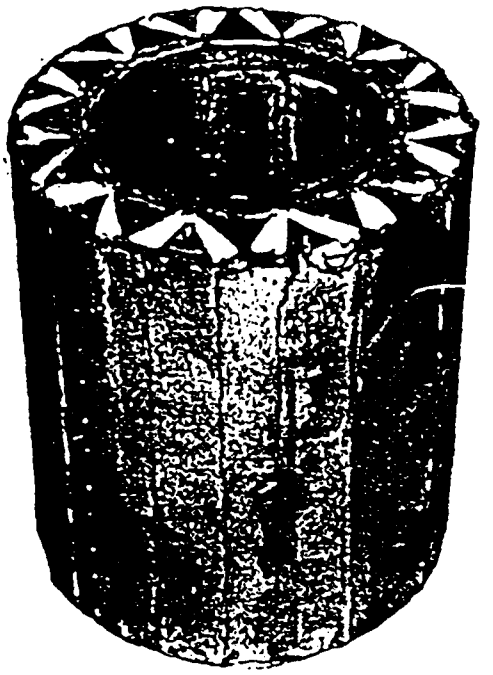

Figure 3-6a EXPLOSIVE CYLINDER CASTING (MODIFIED 12 SIDED CYLINDER)

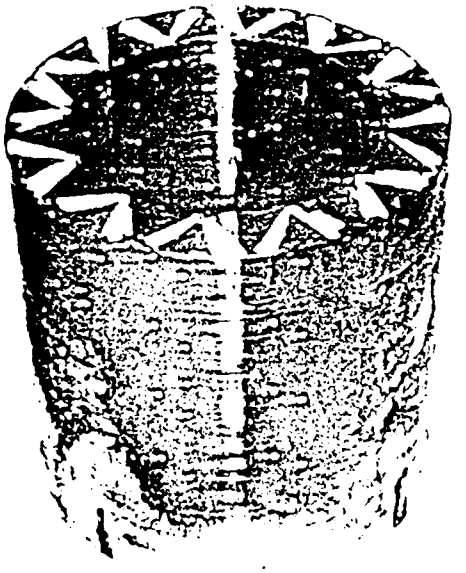

Figure 3-6b MACHINED CYLINDRICAL TEST SPECIMEN

The two warhead cases were delivered for explosive characterization. They both consisted of hollow cylinders with dimensions 11.7 cm (4.6 in.) i.d., 17.3 cm (6.8 in.) o.d. by 15.2 cm (6 in.) long. At Denver Research Institute (DRI), they were hot cast loaded with approximately 4,1 kg. (9 pounds) of Octol 75/25 (HMX/TNT) for arena testing. The exterior surface was covered with 12 rows (30 degrees apart) of tetrahedral and half octahedral fragments weighing approximately 27 grams each.

The total weight of the warhead was 13.6 kg. (30 pounds). A small cavity was machined in the casting for the initiator which consisted of 10 grams of CH-6 booster located at midplane and a commercial No. 8 Vibrodet electric blasting cap inserted in a small central axial hole.

3.2 TEST DESCRIPTION

3.2.1 TEST CONFIGURATION

The two warheads were fired in a vertical position from the top of a support tube eight feet above ground level. The mounted warhead is shown in Figure 3-7. A sketch of the arena layout is shown in Figure 3-8. Six target panels with overall dimensions of 16 feet high by approximately 12 feet wide were located 10 feet from the warhead. For the first test (ETA-1) an extra two feet of panel was used at the bottom of the array extending the total target panel height to 18 feet and allowing for 10 feet above the warhead center. Since this additional height did not appear to be necessary, it was changed for the second test. The target panels consisted of .040" aluminum sheeting (4 feet by 8 feet) and were suspended on a 1.5-inch diameter pipe framework and wired to vertical supports constructed of 2-inch diameter steel pipe located on 4-foot centers. This configuration is illustrated in the photograph in Figure 3.7. The exterior surfaces of the target panels were marked with white lines representing 4-foot square sections as shown in Figure 3-9. For tabulating velocity data, the top halves of the panels were referred to as T and the bottom halves as B (see Figure 3-9).

The fragments in the preform were aimed for each of the tests. For the first test (ETA-1) a row of fragments was aimed at the post in the center of the witness plate and Celotex catcher combination. Two of the fragments actually hit the post resulting in traingular holes. The fragments at the edges of the Celotex catcher panels hit near the edges and exited through the sides of the the catcher panels. The preform in the second test (ETA-2) was rotated 15 deg. and aimed at the center of a witness panel. The effects of this change is found in the data that follows.

Fragment distribution and patterns including cluster orientation were obtained by photographing individual velocity panels after the shot and arranging them in sequential order on a composite print.

Two Fastax cameras were employed to provide complete high-speed photographic coverage of the painted side of the target panels. One full frame camera was operated at approximately 5,000 to 7,000 frames per second and one half-frame camera was operated at 10,000 to 14,000 frames per second.

A separate Celotex fragment recovery pack was used for each test and each pack measured 4 feet wide by 8 feet thick. Each pack was positioned vertically with the front surface located 6 feet from the warhead (see Figures 3-7 and 3-8).

No instrumentation for pressure measurement was used for these test.

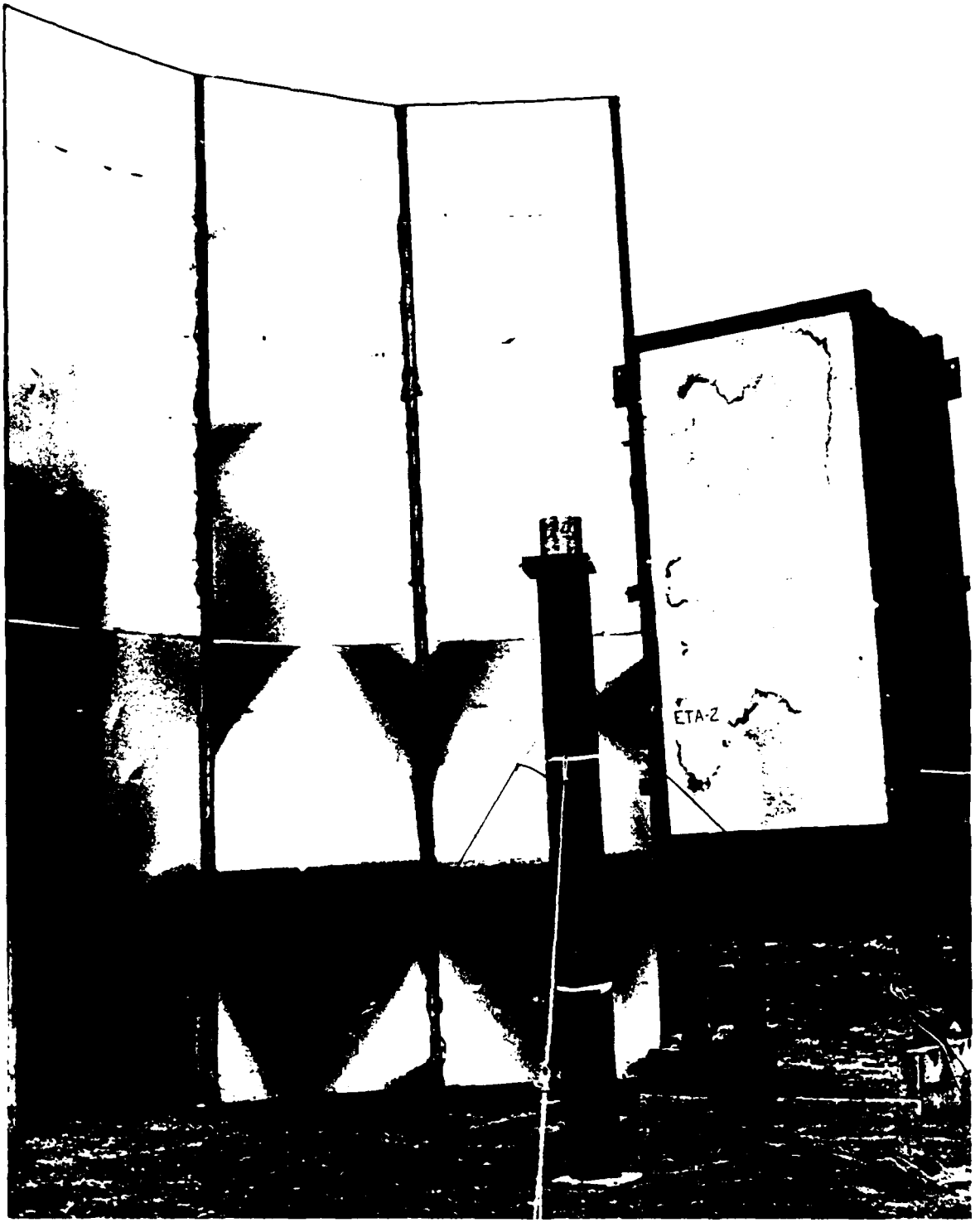

Figure 3-7 WARHEAD MOUNTED IN ARENA

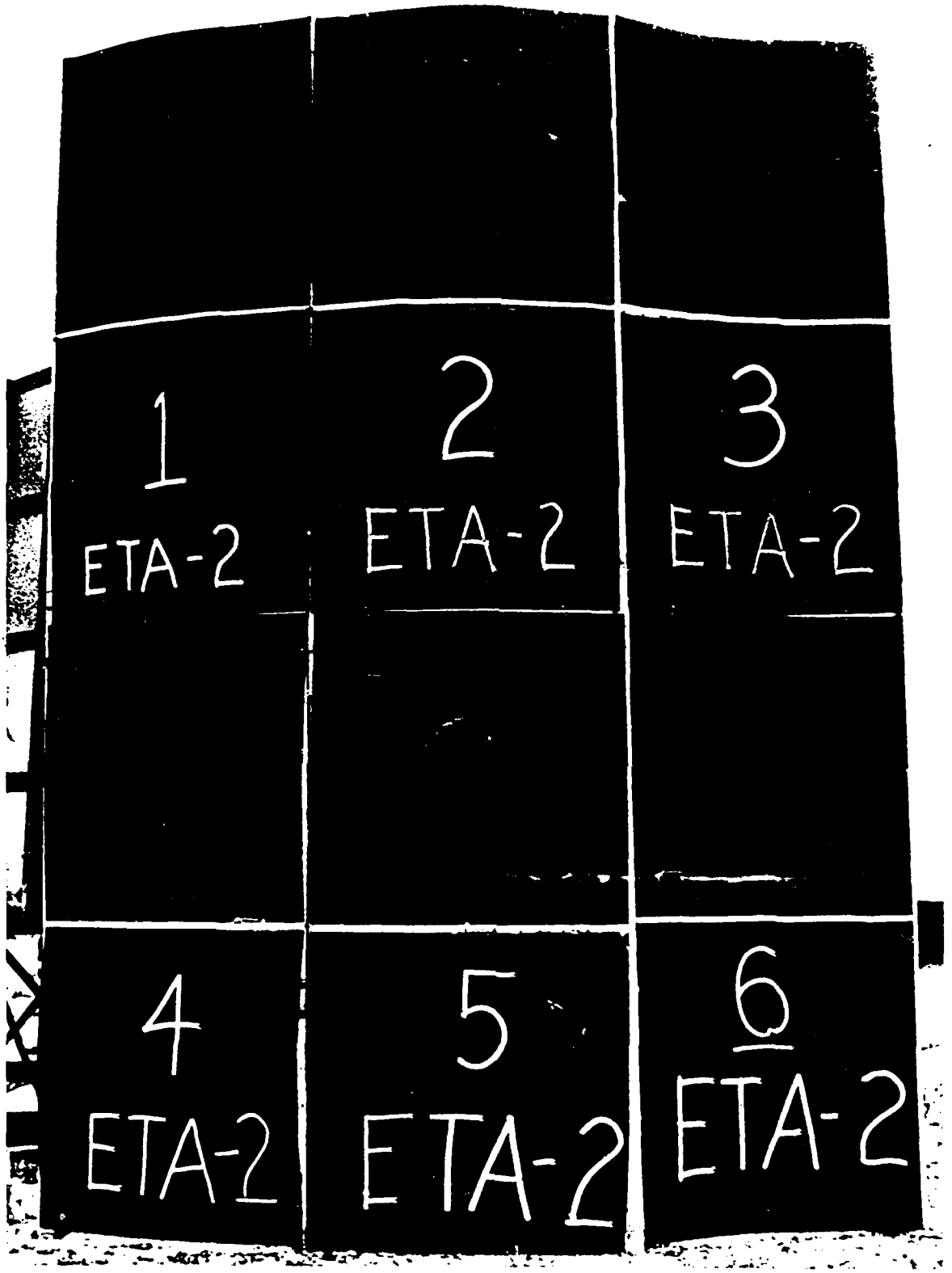

Figure 3-8 ARENA LAYOUT TARGET PANEL CONFIGURATION FOR SHOT ETA-2

3.3 RESULTS AND DISCUSSION

3.3.1 FRAGMENT DISTRIBUTION AND PATTERNS

Fragment distribution and patterns were determined from visual inspection of the target panels, analysis of the high speed film coverage and observation of the celotex fragment recovery pack. Fragment patterns produced on the perforated target panels are shown in the composite prints produced in Figures 3-10 and 3-11 for Test ETA-1 and ETA-2, respectively. The difference in fragment distribution is thought to be the result of changing the aim point between the tests as discussed earlier.

In Figure 3-10 (ETA-1), high density impact areas from three different fragment rows can be observed. Two similar high density regions can be observed in Figure 3-11 for Test ETA-2. Part of another is evident along the right edge of the target panel array. These high density areas were outlined from flash images produced from the high speed film records. In Figures 3-12 and 3-13, tracings of the records were magnified and three separate fragment populations were identified. High density zones associated with early, higher velocity fragments have been outlined and cross hatched. Angular measurements from an approximate center to center print in these zones were made and are indicated in Figures 3-9 and 3-10. These values rage from 28 to 31.5 degrees. Fragment impacts lying outside these primary cluster zones are indicated by solid black circles. Although this population of fragments arrived early and are associated with the outer layer, many of the impact flashes were diminutive in size and brightness, indicative of small fragments (partial fragments).

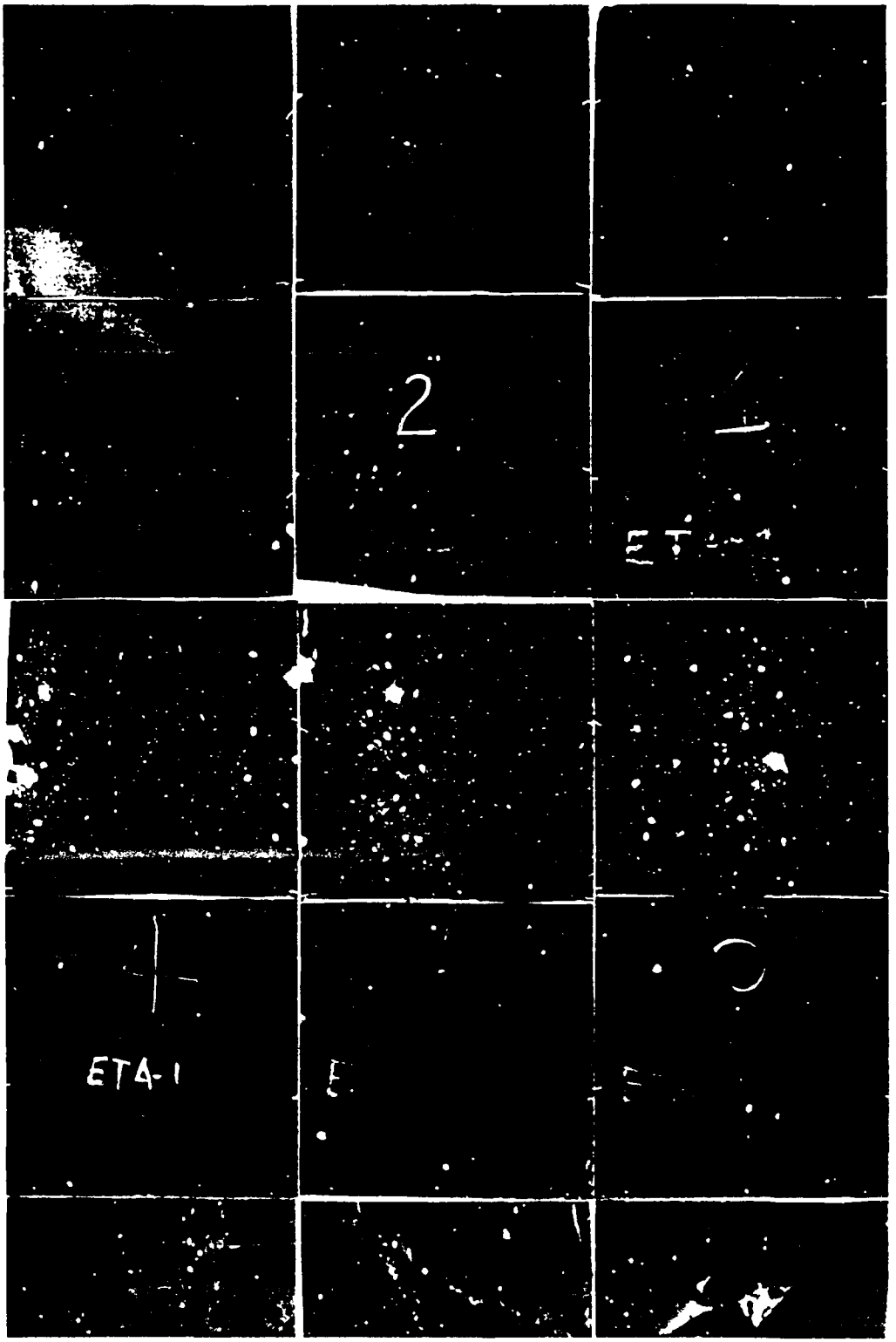

Figure 3-10 COMPOSITE PHOTOGRAPHS OF EXPENDED TARGET PANELS, SHOT ETA-1

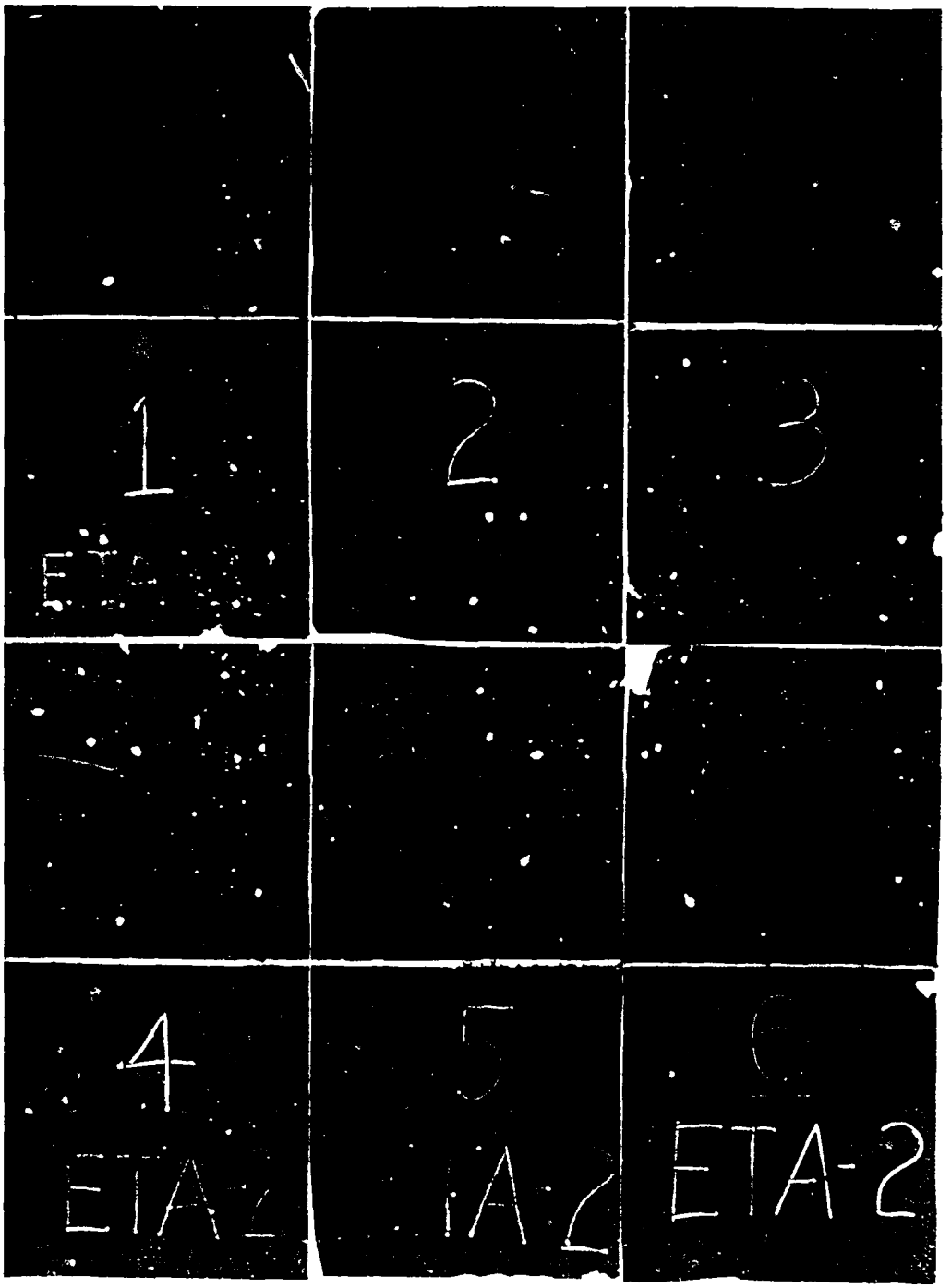

Figure 3-11 COMPOSITE PHOTOGRAPHS OF EXPENDED TARGET PANELS, SHOT ETA-2

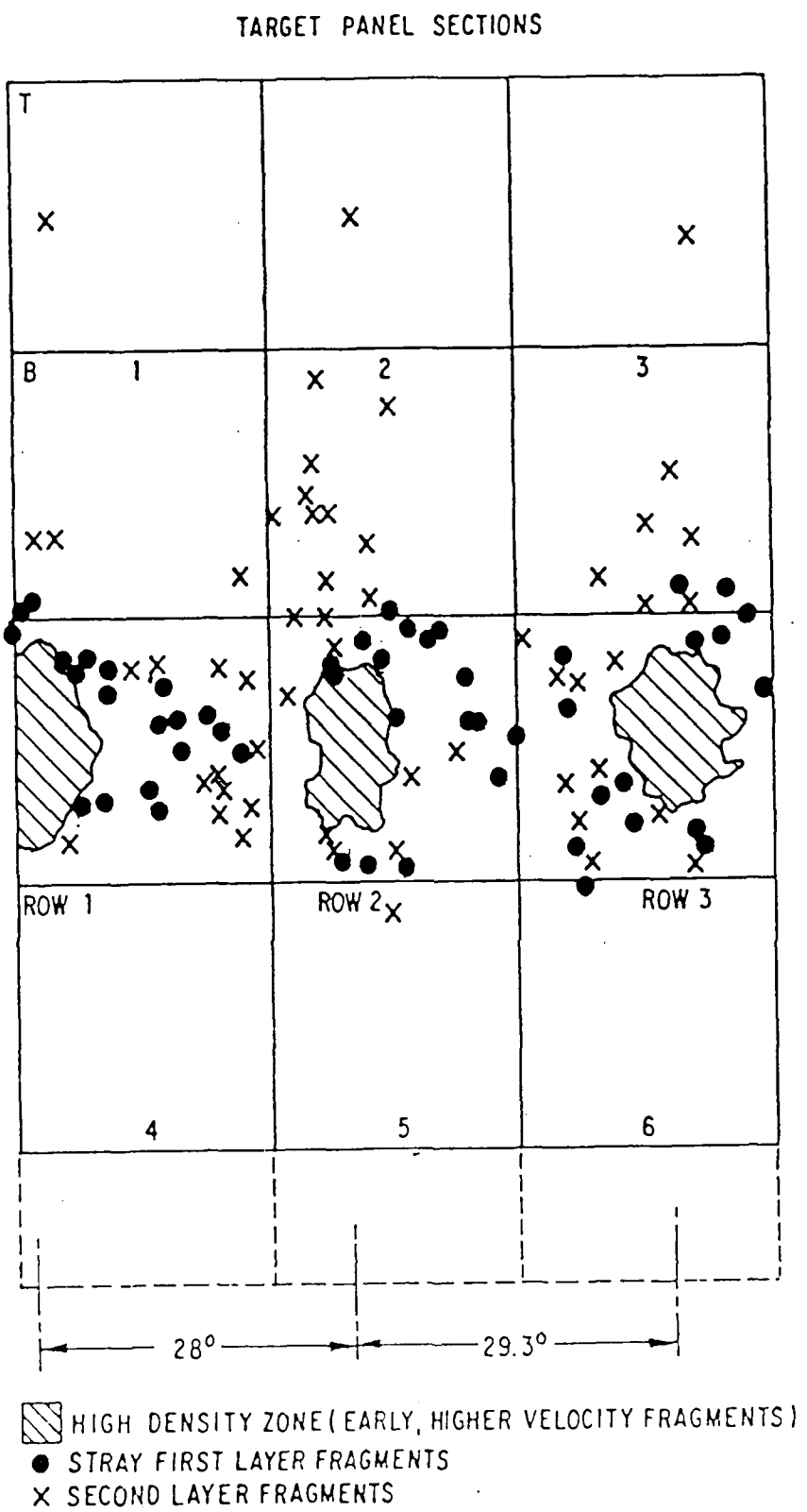

Figure 3-12 TRACING OF TARGET PANELS, ETA-1

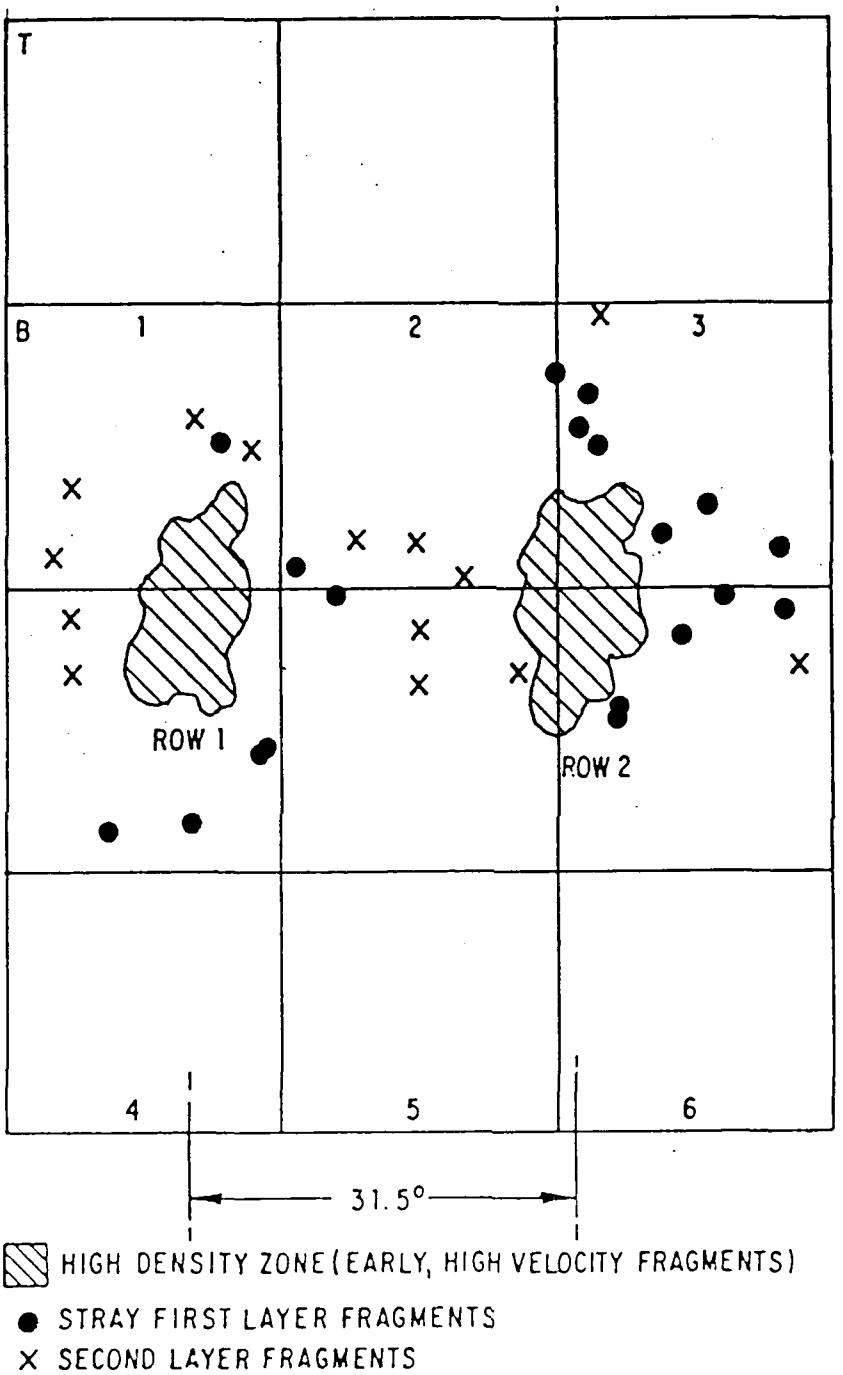

Figure 3-13 TRACING OF TARGET PANELS, ETA-2

Judging by the numbers of impacts from each row, it appears that there was considerable fragment breakup especially among the higher velocity population. The third population of fragments (indicated with x's) is associated with the second fragment layer on the warhead. This group was comprised of primary, integral fragments and partials. The former, represented by bright flashes on the high speed film were approximately ten in number and appeared to the left and somewhat above the high density zones. (See Figures 3-12 and 3-13). In Figure 3-12, ETA-1, the impacts furthest to the left on panel section 4T are only partly shown; the slower fragments were not aligned with the target panel. Looking down on the warhead, the second layer fragments were displaced in a clockwise direction. Average displacements were measured on both target panels and the celotex fragment traps and were approximately 8 and 10.5 degrees for Shots ETA-1 and ETA-2 respectively.

An additional display of fragment distribution can be observed on the celotex recovery pack surface shown in Figures 3-14 and 3-15 for Tests ETA 1 and 2, respectively. For Test ETA-1 (Figure 3-14) only one high density area appeared on the celotex pack surface. However, observe the lower density pattern along the left edge of the pack which is quite similar. The displacement of the second layer fragment population is very well defined here. A high concentration of debris can be observed near the bottom of the pack.

Figure 3-14 CELOTEX PACK AFTER WARHEAD FIRING SHOT ETA-1

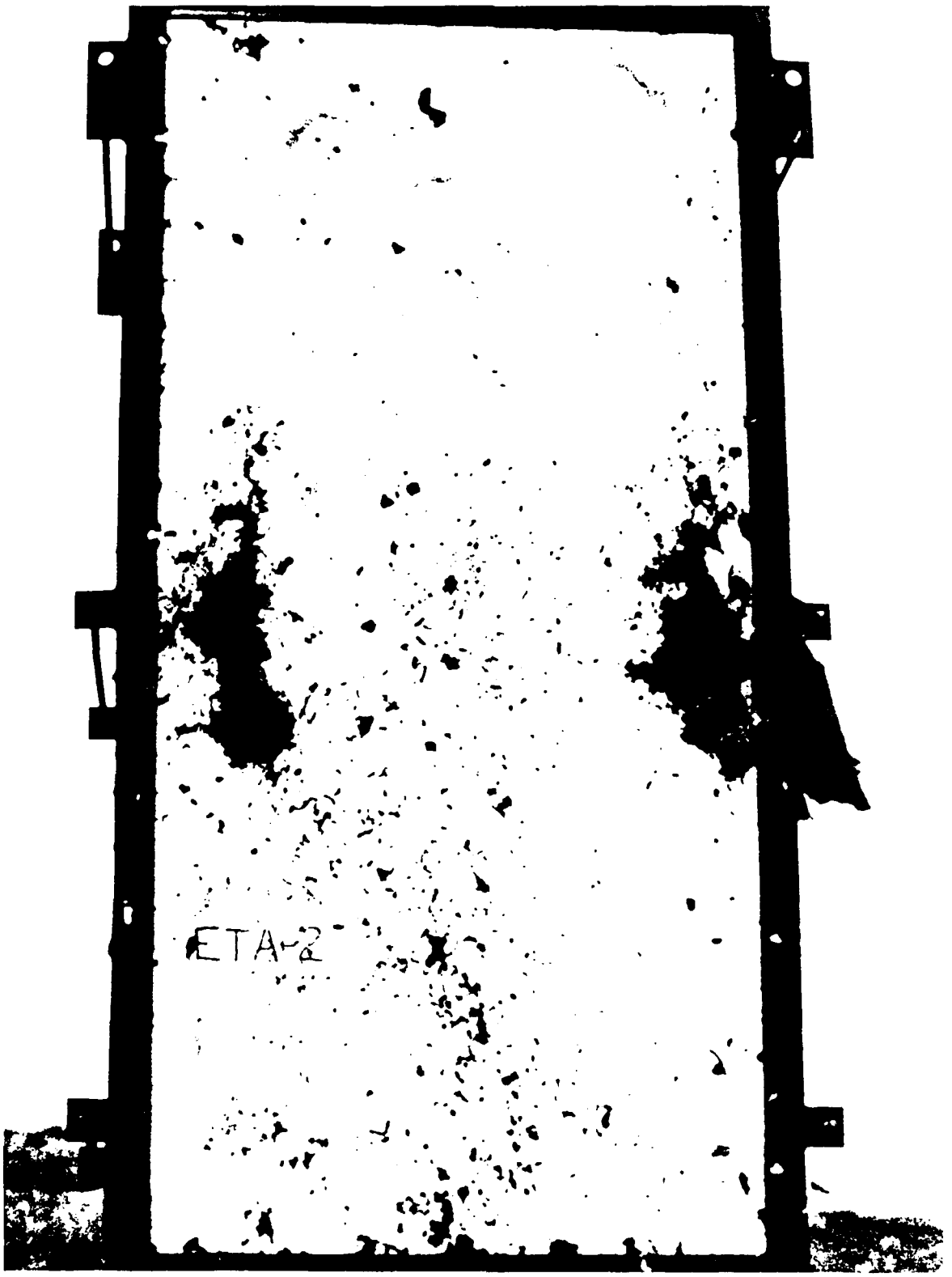

Figure 3-15 CELOTEX PACKS AFTER WARHEAD FIRING, SHOT ETA-2

3.3.2 FRAGMENT VELOCITY ASSESSMENT

Film records from the two Fastax cameras were viewed on a Vanguard Motion Analyzer for determination of average fragment velocities and distribution. This information was obtained using conventional methods involving the observance of fragment impact flashes on the aluminum target panels described earlier. Precise impact positions were recorded as well as film frame numbers counted from warhead first light. The time base for determining the framing rate is obtained from the 1 kHz signal on the margin of the film. From the framing rate, the time interval from warhead breakout (zero time) to fragment impact was determined yielding fragment velocities. Average velocities of both primary (performed) and partials or debris fragments were measured in the manner described and are tabulated in Tables 3-1 and 3-2. The latter category associated with lower intensity flashes are enclosed in parenthesis. Velocities for fragments from the second layer were averaged separately. Fragment totals velocity averages for the entire row are also included. With reference to Table 3-1, ETA-1, maximum velocities were in the range between 1371 m/sec (4500 ft/sec) and 1463 m/sec. (4800 ft/sec). Minimum velocities from the first layer decreased to around 1067 m/sec (3500 ft/sec). Fragment velocities from the second layer raged from around 1036 m/sec (3400 ft/sec) to 762 m/sec (2500 ft/sec). With reference to Table 3-2, ETA-2 results were similar to those obtained for ETA-1. First layer fragment from Row 2 arrived somewhat earlier than those from Row 1. (Compare 1259 m/sec (4130 ft/sec) with 1102 m/sec (3615 ft/sec) for first layer fragments in high density zone). Second layer fragments arrived at about the same time with an average velocity of approximately 914 m/sec (3000 ft/sec). The last fragments of any category to impact the target panels had velocities in the range of 640 m/sec (2100 ft/sec) to 762 m/sec (2500 ft/sec). A summary of the velocities for both shots is presented in Table 3-3.

TABLE 3-1

Individual and Average Fragment Velocities
For Shot ETA-1

Location	Number of Hits	Velocity (ft/sec)	Total Hits	Average Fragment Velocity (ft/sec)
Row 1				
Panel 4T	1 (1)[a]	4850		
	5 (1)	4565		
	7 (1)	4310		
	6 (4)	4085		
	2 (3)	3880		
	1 (3)	3695		
	(7)	3525	22 (20)	4265 (3875)
	2 (6)[b]	3375	2 (6)	3375 (3375)
Panel 1B	(1)[a]	4850	(1)	(4850)
	(1)[b]	3235		
	(1)	2675		
	(3)	2585	(5)	(2735)
Grand Totals - Average			24 (32)	4190 (3635)
Row 2				
Panel 5T	(1)[a]	4850		
	(2)	4565		
	1 (3)	4310		
	5 (6)	4085		
	12 (9)	3880		
	1(10)	3695	19 (36)	3945 (3915)

TABLE 3-1 (cont.)

Location	Number of Hits		Velocity (ft/sec)	Total Hits		Average Fragment Velocity (ft/sec)	
Row 2 (cont'd)							
	4	b	3375				
	3	(2)	3235				
	1	(1)	3105				
	1		2985	9	(3)	3255	(3190)
Panel 4T		(1)a	4085		(1)		(4085)
	4	(3)b	3375				
	3		3235				
		(3)	3105				
		(1)	2985				
	1		2875				
	1		2770	9	(8)	3205	(3315)
Panel 2B		(2)a	3880		(2)		(3880)
		(1)b	3375				
		(2)	3235				
	1		3105				
	1		2985				
	1		2875				
		(3)	2770				
	1		2675				
	1		2585				
	1		2425	6	(6)	2775	(3025)
Panel 1B	1	a	4085	1		4085	
	2	b	2585				
	1		2425	3		2532	
Panel 2T	1	b	3235	1		3235	
Grand Totals - Average				48	(56)	3430	(3695)

TABLE 3-1 (cont.)

Location	Number of Hits	Velocity (ft/sec)	Total Hits	Average Fragment Velocity (ft/sec)
Row 3				
Panel 6T	(1)[a]	4565		
	2 (1)	4310		
	6 (10)	4085		
	6 (2)	3880		
	(7)	3695	14 (21)	4030 (3970)
	(4)[b]	3525		
	4	3375		
	3	3235		
	(3)	3105		
	1 (2)	2985		
	1	2875		
	1	2675		
	(1)	2350	10 (10)	3175 (3175)
Panel 3B	(1)[a]	4085	(1)	(4085)
	(1)[b]	3525		
	1 (3)	3375		
	(1)	3105		
	1	2875		
	2	2675		
	2	2585		
	1	2425	7 (5)	2745 (3350)
Panel 5T	(1)[b]	3525	(1)	(3525)
Panel 6B	(1)[b]	3525	(1)	(3525)
Panel 3T	(1)[b]	2425	(1)	(2425)
Grand Totals - Average			31 (40)	3465 (3635)

---

a Impacts in parentheses were located outside high density region and mostly associated with lower intensity flashes (debris or small fragment pieces)

b Initial impacts from second layer on warhead; lower intensity flashes in parentheses

TABLE 3-2

Individual and Average Fragment Velocities
For Shot ETA-2

Location	Number of Hits	Velocity (ft/sec)	Total Hits		Average Fragment Velocity (ft/sec)	
Row 1						
Panel 4T	(3)[a]	4290				
	1 (4)	3835				
	2	3645				
	2	3470	5	(7)	3615	(4030)
	1 [b]	3170				
	1 (1)	2605	2	(1)	2885	(2605)
Panel 1B	(1)[a]	4290				
	3 (1)	4050				
	3 (2)	3835				
	1	3645				
	1	3470				
	(2)	3315	8	(6)	3845	(3775)
	3 [b]	3170				
	1	2805	4		3080	
Panel 5T	(1)[a]	4290		(1)		(4290)
Panel 2B	(2)[b]	4050		(2)		(4050)
Panel 1T	(1)	2605		(1)		(2605)
Grand Totals - Average			19	(18)	3520	(3805)

TABLE 3-2 (cont.)

Location	Number of Hits	Velocity (ft/sec)	Total Hits	Average Fragment Velocity (ft/sec)	
Row 2					
Panel 3B	(2)[a]	4860			
	1 (1)	4555			
	1	4290			
	(1)	4050			
	2	3835	4 (4)	4130	(4580)
	(2)[b]	3170			
	1	2915			
	1	2700	2 (2)	2810	(3170)
Panel 6T	(2)[a]	4860			
	1	4050			
	1 (1)	3835			
	1	3645	3 (3)	3845	(4520)
	(1)[b]	3315			
	(1)	2805			
	(1)	2085	(3)		(2735)
Panel 2B	1 [a]	4555			
	(1)	3835	1 (1)	4555	(3835)
	1 (1)[b]	3315			
	2	3170			
	1	3040			
	1	2915			
	(1)	2605	5 (2)	3120	(2960)

TABLE 3-2 (cont.)

Location	Number of Hits	Velocity (ft/sec)	Total Hits	Average Fragment Velocity (ft/sec)	
Row 2 (cont'd)					
Panel 5T	1 [a]	4290			
	1	3835			
	1 (1)	3645	3 (1)	3925	(3645)
	1 [b]	3170			
	(1)	2700			
	1	2605	2 (1)	2885	(2700)
Grand Totals - Average			20 (17)	3570	(3680)

---

a Impacts in parentheses were located outside high density region and mostly associated with lower intensity flashes (debris or small fragment pieces)

b Initial impacts from second layer on warhead; lower intensity flashes in parentheses

TABLE 3-3

Summary of Primary Fragment Average Velocities and Row Separation

Shot No.	Row No.	Row Separation (degrees)	Layer Separation (degrees)	Total Impacts Primary Frags
ETA-1	1	---	---	24
	2	28.0	9.5	48
	3	29.3	7.1	31
ETA-2	1	---	10.1	19
	2	31.5	11.1	20

TABLE 3-3 (cont.)

Summary of Primary Fragment Average Velocities and Row Separation

Shot No.	Row No.	Average Frag. 1st Layer	Vel (ft/sec)* 2nd Layer
ETA-1	1	4265	3375
	2	3945	3255
	3	4030	3175
ETA-2	1	3615	2885
	2	4130	2810

* Values from initial impacts in main target panel

3.3.3 FRAGMENT PENETRATION ASSESSMENT

The Celotex catcher sheets were disassembled and the fragements were collected in the various sheets depending upon the fragment penetration. The data was preliminary and could only suggest relationships. In both tests a significant number of the fragments entered the Celotex catcher near the edge and as a result of the radial dispersion the fragments exited through the sides. In ETA-1 the escaping fragments were related to the slower fragments and in ETA-2 the escaping fragments were the faster fragments.

The fragments appeared to have established aerodynamic stability in the short flight time or it was established quickly in the Celotex as their appeared to be no tumbling in the fragments in the catcher material. The fragments left sharply defined triangular paths in the Celotex. Although the data is preliminary it appeared that the penetration was deeper than would have been empirically predicted.

Deeper than expected penetration can be explained by the lack of crushed material in front of the recovered fragments. The tetrahedra presented a tetrahedral tip slightly modified by the torn skin of the tip as shown in Figure 3-15. The half octahedra presented a sharp leading edge formed by the square base and a triangular edge as shown in Figure 3-16. The half-octahedra flew with the triangular surface torn from the skin at its back.

The fragments recovered from the area of massive fragment penetration that had fragment surface markings (the scribe marks put on the cylinders to provide traceability) appeared to be from the same row. The fragments noted earlier as (X) in Figures 3-14 & 15 came from the next row circumferentially.

It appears that the velocity difference between arriving layers 1 and 2 is related to position of the fragment in the casting. Those fragments with their triangular areas exposed to the explosive appeared to have the higher velocities and to have suffered more breakup damage. Those fragments with their triangular exposed area to the outer surface arrived at a lower velocity and with much less fragment break up.

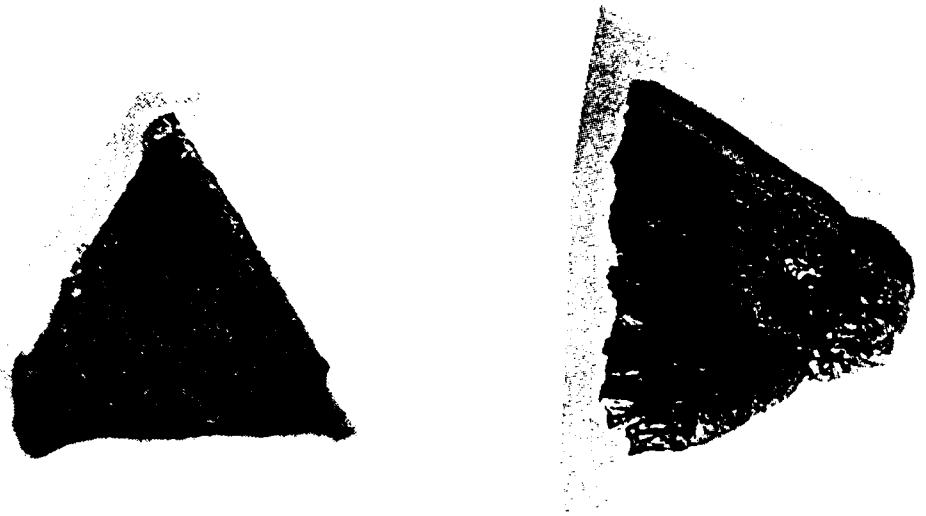

Figure 3-16 TYPICAL TETRAHEDRAL FRAGMENT

Figure 3-17 TYPICAL HALF OCTAHEDRAL FRAGMENT

4.0 CONCLUSIONS AND RECOMMENDATIONS

The preliminary tests were completely successful. It was determined that the multilayered concept will fragment and that the fragments can be dispersed in space and time. In addition, the limited data suggests that the fragments are aerodynamically stable with a leading edge for the half octahedra and a leading point for the tetrahedra. These fragments appeared to penetrate deeper than a comparable mass of chunky (blunt) fragment and they did not appear to tumble in the celotex catcher material. The fragment surfaces immediately next to the explosive appear to have fractured. This potential problem requires more testing to be characterized. If it is a problem, past experience suggests it can be solved with a thin buffering interface layer.

4.1 FRAGMENTATION

The recovery of the fragments in the celutex catcher structure provided an opportunity to evaluate the fragmentation. Although the data is sketchy, the inner layer of fragments which were driven on their flat surface appear to have been damaged by the explosive. There were an number of fractured fragments and fragment pieces in those areas of the catcher associated with the inner flat. In addition, the whole fragments were found with clean skin surfaces representative of the external skin.

These fractured fragments occurred with this explosive and might not have occurred with a less severe explosive. It can be reduced by a thin buffer layer on the inner surface to reduce the sharp leading edge of the explosive. If a future test were carried out it would be recommended to use a layer of attenuator.

The fragmentation test program demonstrated that the concept fragments its skin uniformly and with Octo 72/25 (HMX/TNT) explosive and further developments should include some parameterization of the explosive/skin relationships. These tests would be necessary to bracket the skin structural thicknesses that can be used for designs.

4.2 FRAGMENT DISPERSION

The observation of the witness plates and catchers suggested that the fragments travel in a radial dispersion. The explosive with center initiated so a vertical dispersion was to be expected and it was observed. On first examination of the films, there appeared to be large dispersion angle. Further examination of the catcher and the photographic coverage showed that the dispersion was predominantly the chips and shattered fragments. The dispersion was best shown on the other rows where the fragment dispersion was reasonable for the center initiation.

Further studies should involve core thickness evaluations. The analytic studies suggested that the concept is self sealing, however, this was not demonstrated in these two explosive tests.

4.3 FRAGMENT VELOCITY

The fragment velocities were found in two distributions. The inner cores had an average velocity distribution from 1300 m/sec (4265 ft/sec) to 1102 m/sec (3615 ft/sec) The outer core segment fragments had an average velocity which varied from 1029 m/sec (3375 ft/sec). to 172 m/aec (2810 ft/sec). The difference between the inner and outer core segments is the result of the need to translate the explosive loads through the ceramic spacer wedges. This situation depends very much on the core tooling and the inter fragment ceramic skins.

4.4 FUTURE EFFORTS

Future efforts should first involve testing the remainder of the cylinders to better characterize the results and determine any other characteristics which might not have been observed in these preliminary test.

The observation of of these tests has shown that these fragment geometries appear to be aerodynamically stable and consequently they did not tumble. This was observed in the catcher structure in which the tetrahedrons penetrated with a point forward and the tetrahedrons penetrated with the edge away from the skin a leading edge. In either case the fragments did not tumble and the penetration was significantly deeper than would have been expected for a blunt fragment or a tumbling fragment.

DISTRIBUTION LIST

	No. of Copies
Office of Deputy Under Secretary of Defense for Research and Engineering (ET) ATTN: J. Persh, Staff Specialist for Materials and Structures (Room 3D1089) The Pentagon Washington, DC 20301	1
Office of Deputy Chief of Research Development and Acquisition ATTN: DAMA-CSS The Pentagon Washington, DC 20301	1
Commander U.S. Army Materiel Command ATTN: (AMCSCI, Dr. R. Chait) (Room 10E20) 5001 Eisenhower Avenue Alexandria, VA 22333-0001	1
Strategic Defense Initiative Office ATTN: SLKT, Major R. Yesensky SLKT, A. Young The Pentagon Washington, DC 22304	1 1
Director U.S. Strategic Defense Command ATTN: CSSD-H-QX, D. Bouska CSSD-H-LK, L. Atha CSSD-H-LK, L. Cochran CSSD-H-HA, R. Buckelew CSSD-H-E, J. Katechis CSSD-H-Q, E. Wilkinson CSSD-H-Q, R. Riviera CSSD-H-QE, J. Papadopoulos P.O. Box 1500 Huntsville, AL 35807-3801	1 1 1 1 1 1 1 1

	No. of Copies
Commander U.S. Army Missile Research and Development Command ATTN: DRDMI-EAM, P. Ormsby Redstone Arsenal Huntsville, AL 35809	1
Commander U.S. Army Combat Development Command Institute of Nuclear Studies ATTN: Technical Library Fort Bliss, TX 79916	1
Commander Naval Surface Warfare Center ATTN: J. Foltz Silver Springs, MD 20910	1
Commander U.S. Air Force Wright Aeronautical Laboratories ATTN: AFWAL/FIBAA, A. Gunderson AFWAL/FIBAA, C. R. Waitz AFWAL/MLLS, T. Ronald Wright-Patterson Air Force Base Dayton, OH 45433	1 1 1
Commander BMO/ASMS ATTN: Capt. T. Williams Norton Air Force Base, CA 92409	1
Director Defense Nuclear Agency ATTN: B. Gillis Washington, DC 20305-1000	1
Defense Documentation Center Cameron Station, Bldg. 5 5010 Duke Station Alexandria, VA 22314	2
National Aeronautics and Space Administration ATTN: W. Brewer, Code MS-224 Langley Research Center Hampton, VA 23665	1

	No. of Copies
Institute for Defense Analysis ATTN: Document Control For M. Rigdon 1801 N. Beauregard Street Alexandria, VA 22311	1
Aerospace Corporation ATTN: Document Control For L. McCreight H. Katzman P.O. Box 92957 Los Angeles, CA 90009	1 1
AVCO Systems Division of Textron, Inc. ATTN: Document Control For V. DiCristina 201 Lowell Street Wilmington, MA 01887	1
AVCO Specialty Materials Subsidiary of Textron, Inc. ATTN: Document Control For P. Hoffman M. Mittnick 2 Industrial Avenue Lowell, MA 01851	1 1
The Boeing Aerospace Company ATTN: Document Control For S. Bigelow P. G. Rimbos B. K. Das T. Luhman P. O. Box 3999 Seattle, WA 98124	1 1 1 1
Charles Stark Draper Laboratories ATTN: Document Control For J. Gubbay 555 Technology Avenue Cambridge, MA 02139	1
DWA Composite Specialties, Inc. ATTN: Document Control For J. F. Dolowy, Jr. 21133 Superior Street Chatsworth, CA 91311	1

	No. of Copies
Fiber Materials, Inc. ATTN: Document Control For R. Burns Biddeford Industrial Park Biddeford, ME 04005	1
General Dynamics Corporation Convair Division ATTN: Document Control For J. Hertz K. Meyer P. O. Box 80847 San Diego, CA 92130	1 1
General Electric Company Advanced Materials Development Laboratory ATTN: Document Control For J. Brazel K. Hall 3198 Chestnut Street Philadelphia, PA 19101	1 1
General Electric Company Valley Forge Space Center ATTN: Document Control For C. Zweben P. O. Box 8555 Philadelphia, PA 19101	1
General Research Corporation ATTN: Document Control For J. Green P. O. Box 6770 5383 Hollister Avenue Santa Barbara, CA 93111	1
Kaman Tempo ATTN: Document Control For L. Gonzalez 816 State Street Santa Barbara, CA 93101	1
Lockheed-Georgia Company ATTN: Document Control For J. Carroll W. Bates 86 South Cobb Drive Marietta, GA 30063	1 1

	No. of Copies
Lockheed Missiles and Space Company	
ATTN: Document Control	
For W. Loomis	1
D. Himmelblau	1
R. Torczyner	1
H. Chang	1
1111 Lockheed Way	
Sunnyvale, CA 94089	
Martin Marietta Orlando Aerospace	
ATTN: Document Control	
For R. Caime	1
K. Hanson	1
F. Koo	1
M. Hendricks	1
P.O. Box 5837	
Orlando, FL 32805	
Martin Marietta Baltimore Aerospace	
ATTN: Document Control	
For W. Couch	1
103 Chesapeake Park Plaza	
Baltimore, MD 21220	
Martin Marietta Denver Aerospace	
ATTN: Document Control	
For M. Misra	1
P. O. Box 179	
Denver, CO 80201	
Material Concepts, Inc.	
ATTN: Document Control	
For D. Kizer	1
666 North Hague Avenue	
Columbus, OH 43204	
McDonnell Douglas Astronautics Company	
ATTN: Document Control	
For J. Ditto	1
J. Davidson	1
J. Grossman	1
H. Parachanian	1
B. Leonard	1
5301 Bolsa Avenue	
Huntington Beach, CA 92647	

	No. of Copies
PDA Engineering ATTN: Document Control For M. Sherman 2975 Red Hill Avenue Costa Mesa, CA 92626	1
Rohr Industries, Inc. ATTN: Document Control For N. R. Adsit Foot of H Street P. O. Box 878 Chula Vista, CA 92012-0878	1
SPARTA, Inc ATTN: Document Control For J. Glatz G. Wonacott 1055 Wall Street, Suite 200 P.O. Box 1354 La Jolla, CA 92038	1 1
SPARTA, Inc. ATTN: Document Control For I. Osofsky 3440 Carson Street, Suite 300 Torrance, CA 90503	1
SPARTA, Inc. ATTN: Document Control For D. Weisinger 1104B Camino Del Mar Del Mar, CA 92014	1
Southwest Research Institute ATTN: Document Control For A. Wenzel 8500 Culebra Road San Antonio, TX 78206	1
Stone Engineering Co. ATTN: Document Control For W. Stone 805 Madison Street, Suite 2C Huntsville, AL 35801	1

	No. of Copies
Teledyne Brown Engineering ATTN: Document Control For C. Patty Research Park 300 Sparkman Drive Huntsville, AL 35807	1
Director Army Materials Technology Laboratory	
ATTN: SLCMT-BM, J. F. Dignam	1
SLCMT-BM, L. R. Aronin	1
SLCMT-MRD, S. C. Chou	1
SLCMT-ISC	1
SLCMT-IML Watertown, MA 02172-0001	2

U. S. Army Materials Technology Laboratory
Watertown, MA 02172-0001
A STUDY OF FRAGMENTATION DISPERSION MEASUREMENTS UNIQUE MULTILAYER FRAGMENTING STRUCTURE
D. L. Mykkanen
ETA Corporation
18301 Churchill Ln.
Villa Park, CA 92667
Technical Report MTL TR 89-7
55 pp-illus,-tables, Contract DAAG46-85-C-0078
D/A Project: 8X363304D215, AMCMS Code: P693000.215
Final Report, September 26, 1985 - June 26, 1987

AD____________________
UNCLASSIFIED
UNLIMITED DISTRIBUTION

Key Words
Warheads
Fragmentation
Investment casting
Structural elements
Explosive testing

This experimental program demonstrated the fragmentation feasibility of an integrated multilayered fragmenting warhead structure which uses the fragment mass to increase the structural strength and stiffness and then uses the structural weight as deliverable fragment mass. The fabrication techniques and design developments were accomplished using lost wax technology employing ceramic cores to separate the fragments during the casting of a 17-4PH steel cylindrical concept. Modified cylinders (12 sided polygons) were cast and cylindrical explosive test specimens were machined. The explosive fragmentation tests used cast cylinders filled with explosive which was then center point initiated. The fragments were characterized with aluminum witness plates to determine the velocity and fiber board catchers to establish the fragment integrity. The tests demonstrated that the total structure of the integrated structure/warhead concept can be explosively fragmented. The fragments generated will penetrate to great depths made possibly as a result of their being tetrahedral or octahedral shapes and their apparent aerodynamic stability. Additional work needs to be done to gather data to produce the technology for system design application.

U. S. Army Materials Technology Laboratory
Watertown, MA 02172-0001
A STUDY OF FRAGMENTATION DISPERSION MEASUREMENTS UNIQUE MULTILAYER FRAGMENTING STRUCTURE
D. L. Mykkanen
ETA Corporation
18301 Churchill Ln.
Villa Park, CA 92667
Technical Report MTL TR 89-7
55 pp-illus,-tables, Contract DAAG46-85-C-0078
D/A Project: 8X363304D215, AMCMS Code: P693000.215
Final Report, September 26, 1985 - June 26, 1987

AD____________________
UNCLASSIFIED
UNLIMITED DISTRIBUTION

Key Words
Warheads
Fragmentation
Investment casting
Structural elements
Explosive testing

This experimental program demonstrated the fragmentation feasibility of an integrated multilayered fragmenting warhead structure which uses the fragment mass to increase the structural strength and stiffness and then uses the structural weight as deliverable fragment mass. The fabrication techniques and design developments were accomplished using lost wax technology employing ceramic cores to separate the fragments during the casting of a 17-4PH steel cylindrical concept. Modified cylinders (12 sided polygons) were cast and cylindrical explosive test specimens were machined. The explosive fragmentation tests used cast cylinders filled with explosive which was then center point initiated. The fragments were characterized with aluminum witness plates to determine the velocity and fiber board catchers to establish the fragment integrity. The tests demonstrated that the total structure of the integrated structure/warhead concept can be explosively fragmented. The fragments generated will penetrate to great depths made possibly as a result of their being tetrahedral or octahedral shapes and their apparent aerodynamic stability. Additional work needs to be done to gather data to produce the technology for system design application.

U. S. Army Materials Technology Laboratory
Watertown, MA 02172-0001
A STUDY OF FRAGMENTATION DISPERSION MEASUREMENTS UNIQUE MULTILAYER FRAGMENTING STRUCTURE
D. L. Mykkanen
ETA Corporation
18301 Churchill Ln.
Villa Park, CA 92667
Technical Report MTL TR 89-7
55 pp-illus,-tables, Contract DAAG46-85-C-0078
D/A Project: 8X363304D215, AMCMS Code: P693000.215
Final Report, September 26, 1985 - June 26, 1987

AD____________________
UNCLASSIFIED
UNLIMITED DISTRIBUTION

Key Words
Warheads
Fragmentation
Investment casting
Structural elements
Explosive testing

This experimental program demonstrated the fragmentation feasibility of an integrated multilayered fragmenting warhead structure which uses the fragment mass to increase the structural strength and stiffness and then uses the structural weight as deliverable fragment mass. The fabrication techniques and design developments were accomplished using lost wax technology employing ceramic cores to separate the fragments during the casting of a 17-4PH steel cylindrical concept. Modified cylinders (12 sided polygons) were cast and cylindrical explosive test specimens were machined. The explosive fragmentation tests used cast cylinders filled with explosive which was then center point initiated. The fragments were characterized with aluminum witness plates to determine the velocity and fiber board catchers to establish the fragment integrity. The tests demonstrated that the total structure of the integrated structure/warhead concept can be explosively fragmented. The fragments generated will penetrate to great depths made possibly as a result of their being tetrahedral or octahedral shapes and their apparent aerodynamic stability. Additional work needs to be done to gather data to produce the technology for system design application.

U. S. Army Materials Technology Laboratory
Watertown, MA 02172-0001
A STUDY OF FRAGMENTATION DISPERSION MEASUREMENTS UNIQUE MULTILAYER FRAGMENTING STRUCTURE
D. L. Mykkanen
ETA Corporation
18301 Churchill Ln.
Villa Park, CA 92667
Technical Report MTL TR 89-7
55 pp-illus,-tables, Contract DAAG46-85-C-0078
D/A Project: 8X363304D215, AMCMS Code: P693000.215
Final Report, September 26, 1985 - June 26, 1987

AD____________________
UNCLASSIFIED
UNLIMITED DISTRIBUTION

Key Words
Warheads
Fragmentation
Investment casting
Structural elements
Explosive testing

This experimental program demonstrated the fragmentation feasibility of an integrated multilayered fragmenting warhead structure which uses the fragment mass to increase the structural strength and stiffness and then uses the structural weight as deliverable fragment mass. The fabrication techniques and design developments were accomplished using lost wax technology employing ceramic cores to separate the fragments during the casting of a 17-4PH steel cylindrical concept. Modified cylinders (12 sided polygons) were cast and cylindrical explosive test specimens were machined. The explosive fragmentation tests used cast cylinders filled with explosive which was then center point initiated. The fragments were characterized with aluminum witness plates to determine the velocity and fiber board catchers to establish the fragment integrity. The tests demonstrated that the total structure of the integrated structure/warhead concept can be explosively fragmented. The fragments generated will penetrate to great depths made possibly as a result of their being tetrahedral or octahedral shapes and their apparent aerodynamic stability. Additional work needs to be done to gather data to produce the technology for system design application.